THE JOURNAL OF BIOLOGICAL CHEMISTRY VOL. 291, NO. 34, pp. 17754–17771, August 19, 2016

Twin Attributes of Tyrosyl-tRNA Synthetase of *Leishmania donovani*

*A HOUSEKEEPING PROTEIN TRANSLATION ENZYME AND A MIMIC OF HOST CHEMOKINE**

Received for publication, March 12, 2016, and in revised form, July 1, 2016 Published, JBC Papers in Press, July 5, 2016, DOI 10.1074/jbc.M116.727107

Sneha Anand[1] **and Rentala Madhubala**[2]

From the School of Life Sciences, Jawaharlal Nehru University, New Delhi 110067, India

Aminoacyl-tRNA synthetases (aaRSs) are housekeeping enzymes essential for protein synthesis. Apart from their parent aminoacylation activity, several aaRSs perform non-canonical functions in diverse biological processes. The present study explores the twin attributes of *Leishmania* tyrosyl-tRNA synthetase (*Ld*TyrRS) namely, aminoacylation, and as a mimic of host CXC chemokine. *Leishmania donovani* is a protozoan parasite. Its genome encodes a single copy of tyrosyl-tRNA synthetase. We first tested the canonical aminoacylation role of *Ld*TyrRS. The recombinant protein was expressed, and its kinetic parameters were determined by aminoacylation assay. To study the physiological role of *Ld*TyrRS in *Leishmania*, gene deletion mutations were attempted via targeted gene replacement. The heterozygous mutants showed slower growth kinetics and exhibited attenuated virulence. *Ld*TyrRS appears to be an essential gene as the chromosomal null mutants did not survive. Our data also highlights the non-canonical function of *L. donovani* tyrosyl-tRNA synthetase. We show that *Ld*TyrRS protein is present in the cytoplasm and exits from the parasite cytoplasm into the extracellular medium. The released *Ld*TyrRS functions as a neutrophil chemoattractant. We further show that *Ld*TyrRS specifically binds to host macrophages with its ELR (Glu-Leu-Arg) peptide motif. The ELR-CXCR2 receptor interaction mediates this binding. This interaction triggers enhanced secretion of the proinflammatory cytokines TNF-α and IL-6 by host macrophages. Our data indicates a possible immunomodulating role of *Ld*TyrRS in *Leishmania* infection. This study provides a platform to explore *Ld*TyrRS as a potential target for drug development

Aminoacyl-tRNA synthetases (aaRSs)[3] are the central. enzymes in protein translation, providing charged tRNAs for the appropriate construction of peptide chains. The canonical function of aaRSs is to charge specific tRNAs with their cognate amino acids and thereby contribute to accurate mRNA translation during protein synthesis. Thus, aaRSs are essential components of protein synthesis in every living species.

Apart from their basic function of charging tRNA molecules for protein synthesis, non-canonical functions like ribosomal RNA biogenesis, angiogenesis, apoptosis, transcriptional regulation, and cell signaling have also been reported for several aaRSs (1, 2). Novel functions of this group of enzymes depend on the addition of one or more new domains or motifs during the course of evolution (3).

Tyrosyl-tRNA synthetase (TyrRS) is one such aaRS, which belong to a family of class I synthetases, characterized by a structurally well conserved amino-terminal Rossmann-fold domain, which contains the signature sequences "HIGH" and "KMSKS." The mammalian TyrRS contains a closely homologous endothelial monocyte activating polypeptide II (EMAPII) domain at the C terminus (4). Under specific conditions, human TyrRS is processed by an elastase enzyme into a free carboxyl-terminal EMAPII-like domain and a second amino-terminal part known as mini-TyrRS. Both released proteins are active in distinct immune signaling pathways (4, 5). The carboxyl-terminal domain of human TyrRS mimics the cytokine function of EMAPII. On the other hand, human mini-TyrRS, via its ELR (Glu-Leu-Arg) motif, interacts with the CXC-chemokine receptor (CXCR1/2), and like IL-8, functions as a chemoattractant for polymorphonuclear leukocytes (4, 5). The ELR motif is a signature motif of CXC chemokines such as IL-8 that are active as polymorphonuclear leukocyte chemoattractants (6). This motif is essential for receptor binding and the chemotactic activity of CXC chemokines (7–9). The ELR motif in mini-TyrRS is also important for its chemokine-like activity (4, 5). This data on human TyrRS suggests that the twin attributes of chemokine trigger and aminoacylation coexist in TyrRS.

Not much is known about aaRSs in *Leishmania* sp. *Leishmania* genus is the causative agent of leishmaniasis, a group of neglected diseases. The clinical symptoms of the disease depend on the species involved. *Leishmania* has a digenetic life cycle. Infected sand flies inoculate the mammalian host with promastigotes. Within the mammalian host, promastigotes differentiate into amastigotes that replicate in phagolysosomes. *Leishmania* parasites have the capability of subverting host function, thereby allowing the parasite to thrive within the organism (10, 11). The development of resistance to currently available anti-leishmanial drugs has led to an urgent need to

* This work was supported in part by Department of Biotechnology, Government of India Grant 102/IFD/SAN/3321/2014–15 (to R. M.). The authors declare that they have no conflicts of interest with the contents of this article.

[1] Recipient of funding from the University Grants Commission, India.

[2] JC Bose National Fellow. To whom correspondence should be addressed. Tel./Fax: 91-11-26742630; E-mail: rentala@outlook.com.

[3] The abbreviations used are: aaRS, aminoacyl-tRNA synthetases; TyrRS, tyrosyl-tRNA synthetase; *Ld*TyrRS, *L. donovani* TyrRS; $tRNA^{Tyr}$, tyrosyl-$tRNA^{Tyr}$; EMAPII, endothelial monocyte activating polypeptide II domain; fMLP, formylmethionyl-leucyl-phenylalanine; ELR/AAA, mutant *Ld*TyrRS protein in which ELR motif has been mutated to AAA; r*Ld*LeuRS, recombinant *L. donovani* leucyl-tRNA synthetase.

discover novel drug targets (12). In this regard, aaRSs constitute ideal targets for drug development.

The crystal structure of *Leishmania major* TyrRS has been recently solved, and it is known to exist as an asymmetric pseudodimer (13). In the present study, we report the catalytic promiscuity and moonlighting function of *L. donovani* TyrRS (*Ld*TyrRS). The twin attributes of *L. donovani* tyrosyl-tRNA synthetase, namely, aminoacylation and chemokine trigger have been determined. Our earlier comprehensive bioinformatic analysis led to the identification of a total of 26 aaRSs in *Leishmania* (14). The *Leishmania* genome encodes a single copy of TyrRS (tritrypDB ID LdBPK_141460.1). The present study characterizes the aminoacylation activity of *Ld*TyrRS. To elucidate the physiological role of *Ld*TyrRS, gene deletion mutations were attempted via targeted gene replacement. Heterozygous knock-out mutants of *LdTyrRS* showed reduced growth and were attenuated in their infectivity, indicating the essentiality of this protein. Several attempts to generate homozygous null mutants of *LdTyrRS* were unsuccessful due to the presence of a single copy of the *TyrRS* gene. Fisetin, a natural flavonoid compound, was found to inhibit parasite growth by inhibiting the aminoacylation activity of *LdTyrRS*. Apart from its role in translation, we also report the non-canonical function of *LdTyrRS.* The most notable and intriguing feature of *Ld*TyrRS is the presence of an "ELR" motif, which is the signature motif conserved among IL-8 chemokines (15) and indicates a possible immunomodulating role of this protein. We explored the significance of this ELR motif in the parasite housekeeping enzyme *Ld*TyrRS. Our comprehensive study involving the characterization, localization, and immunological attributes of *Ld*TyrRS provides a platform to explore *LdTyrRS* as a potential target for drug development.

Results

Characterization of Leishmania Tyrosyl-tRNA Synthetase (LdTyrRS)—Multiple sequence alignment of *Ld*TyrRS (Uniprot ID A4HW83; tritrypDB ID LdBPK_141460.1) with representative sequences from other eukaryotes such as human (Uniprot ID P54577), *Plasmodium* (UniProt ID Q8IAR7), *Trypanosoma brucei* (Uniprot ID Q57WH7; tritrypDB ID Tb927.7.3620), and *L. major* (Uniprot ID Q4QFJ7; tritrypDB ID LMJF_14_1370) was generated using CLUSTALW. This multiple sequence alignment showed that *Ld*TyrRS belongs to a family of class I synthetases, characterized by a structurally well conserved amino-terminal Rossmann-fold domain that contains the signature sequences HIGH and KMSKS. Our earlier bioinformatics analysis has revealed the presence of an "ELR (Glu-Leu-Arg) motif," which is the signature motif conserved among CXC chemokines (14). The ELR motif in *Ld*TyrRS was found to be present at the 22nd amino acid position and indicated a possible immunomodulating role of this enzyme (Fig. 1). The alignment also suggested complete conservation of the ELR motif in parasitic tyrosyl-tRNA synthetases (*Plasmodium*, *T. brucei,* and *L. major*). Interestingly, the ELR motif was found to be evolutionarily absent in TyrRSs from lower eukaryotes and prokaryotes (Fig. 2).

To characterize the recombinant *Ld*TyrRS protein, the full-length gene was cloned into a bacterial expression vector pET30a. A histidine-tagged fusion protein with an estimated molecular mass of ~80 kDa was induced. This size correlated with the amino acid composition of the *Ld*TyrRS protein (~74 kDa) with a His_6 tag (~6 kDa) at the N terminus (Fig. 3*A*). Recombinant *Ld*TyrRS was purified to homogeneity by metal affinity chromatography (Fig. 3*A*). Purification yielded ~2 mg of purified protein/liter of bacterial culture. The recombinant protein (r*Ld*TyrRS) was recognized by an anti-His tag monoclonal antibody (Fig. 3*B*). To further characterize r*Ld*TyrRS, the purified protein was analyzed by MALDI-TOF/TOF mass spectroscopy (data not shown). The spectrum of the protein analyzed by BioTools version 2.2 showed an intensity coverage of 46.6% for tyrosyl-tRNA synthetase (*Leishmania infantum*). The expression of the full-length *Ld*TyrRS enzyme was confirmed in *Leishmania* cell lysates by immunoblot analysis (Fig. 3*C*). The anti-*Ld*TyrRS antibody detected a ~74 kDa band in the cell extracts of both the promastigotes and the amastigotes (Fig. 3*C*).

Enzymatic Activity and Kinetic Parameters for LdTyrRS—To assess the aminoacylation activity of r*Ld*TyrRS, a coupled enzyme assay was performed. The aminoacylation reaction was carried out with r*Ld*TyrRS in the presence of inorganic pyrophosphatase, and the P_i produced was measured with a malachite green solution. Recombinant *Ld*TyrRS acylated $tRNA^{Tyr}$ in a time-dependent manner, demonstrating that the *L. donovani TyrRS* gene encodes a functional enzyme (Fig. 3*D*). The kinetic parameters and specificity of r*Ld*TyrRS were determined with L-tyrosine and $tRNA^{Tyr}$ as substrates *in vitro* (Fig. 3, *E* and *F*). Enzyme kinetics was performed with varying concentrations of L-tyrosine (from 0.1 to 20 μM), whereas other components were kept constant (Fig. 3*E*). The results showed that the enzyme reaction was dependent on L-tyrosine concentration (Fig. 3*E*). The K_m value of r*Ld*TyrRS for L-tyrosine was 0.21 ± 0.0245 μM, which is closer to that reported in the case of human TyrRS (0.3 μM) (16). Because $tRNA^{Tyr}$ is another essential substrate of the aminoacylation reaction, therefore, we also performed $tRNA^{Tyr}$-dependent enzyme kinetics studies (Fig. 3*F*). The estimated K_m of *Ld*TyrRS, for $tRNA^{Tyr}$ (1.177 ± 0.2271 μM), was closer to that of humans (0.9 μM) (16) but higher than that of *Saccharomyces cerevisiae* (0.2 μM) (17).

Subcellular Localization of LdTyrRS—The amino acid sequence analysis of *Ld*TyrRS by web-based programs like signalP and pSORT II predicted that *Ld*TyrRS does not contain any detectable signal peptide or cleavage site. Moreover, predictions with MARSPred and LocTree3 also indicated a preferentially cytosolic localization. To ascertain the localization of TyrRS in *L. donovani*, immunofluorescence analysis of log phase promastigotes stained with anti-*Ld*TyrRS antibody and DAPI was conducted. The kinetoplast and nuclear DNA in these cells were readily identified by their bright staining with DAPI (Fig. 4*B*). *Ld*TyrRS was found to be localized only in the cytoplasm of the parasite (Fig. 4, *C* and *D*). Earlier data from mass spectrometry has demonstrated a predominantly cytoplasmic localization of TyrRS in *T. brucei* (18). Controls performed with mouse preimmune sera, non-permeabilized cells, and secondary antibody alone showed no detectable signal (data not shown).

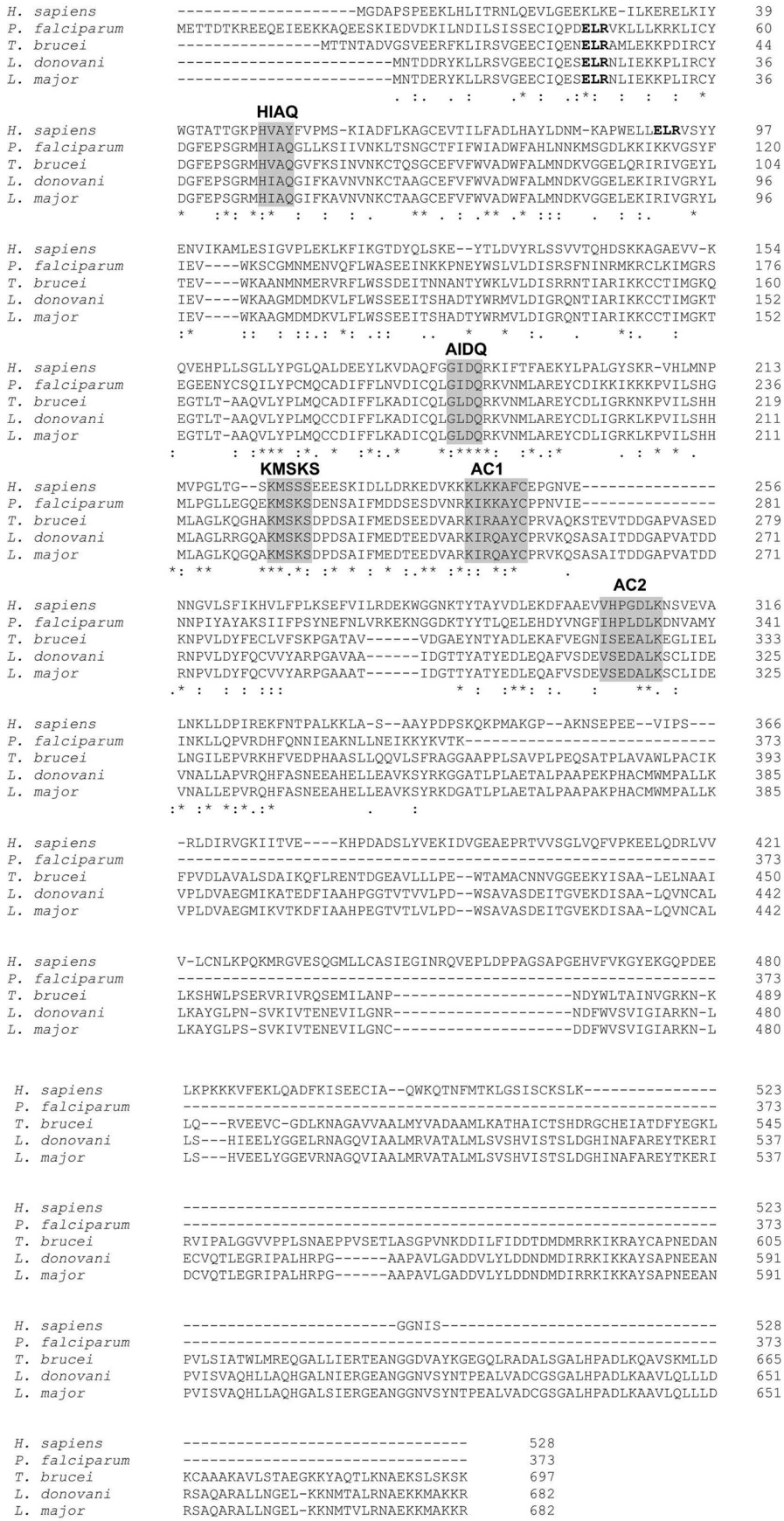

FIGURE 1. **Multiple sequence alignment of representative TyrRS sequences from kinetoplastids, human, and *Plasmodium* species generated using CLUSTALW.** The key residues present in the aminoacylation and catalytic domains are highlighted in a *gray background*. The ELR motif is highlighted in *bold font*.

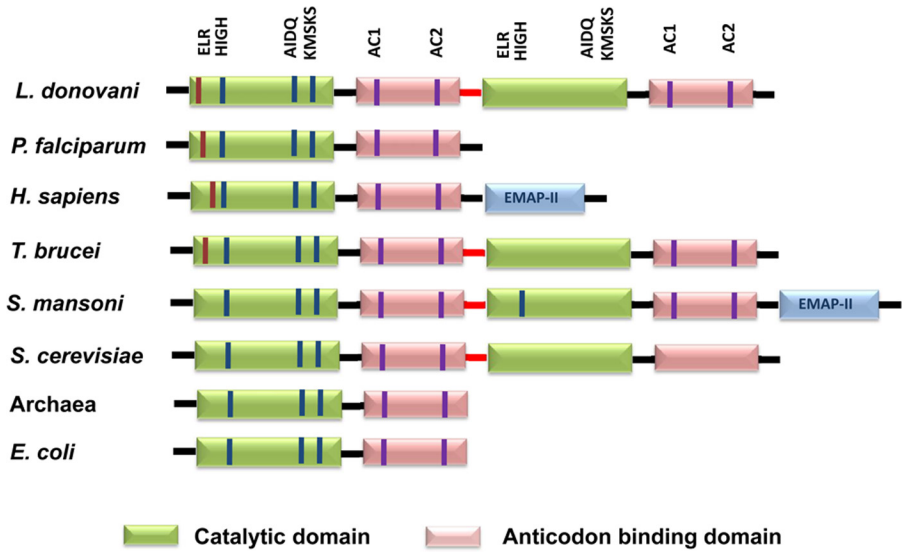

FIGURE 2. **Domain organization of TyrRS from eukaryotes and prokaryotes.** The catalytic and anticodon binding domains are indicated. The ELR motif is present at the N terminus and is shown in *red*. The HIGH and KMSKS active site motifs are common to all class I catalytic domains. The AIDQ motif is characteristic of the ATP binding site in TyrRS. The AC1 motif corresponds to the anticodon-binding domain that interacts with the anticodon stem of $tRNA^{Tyr}$. The AC2 motif specifically recognizes the anticodon bases G34 and U/ψ35.

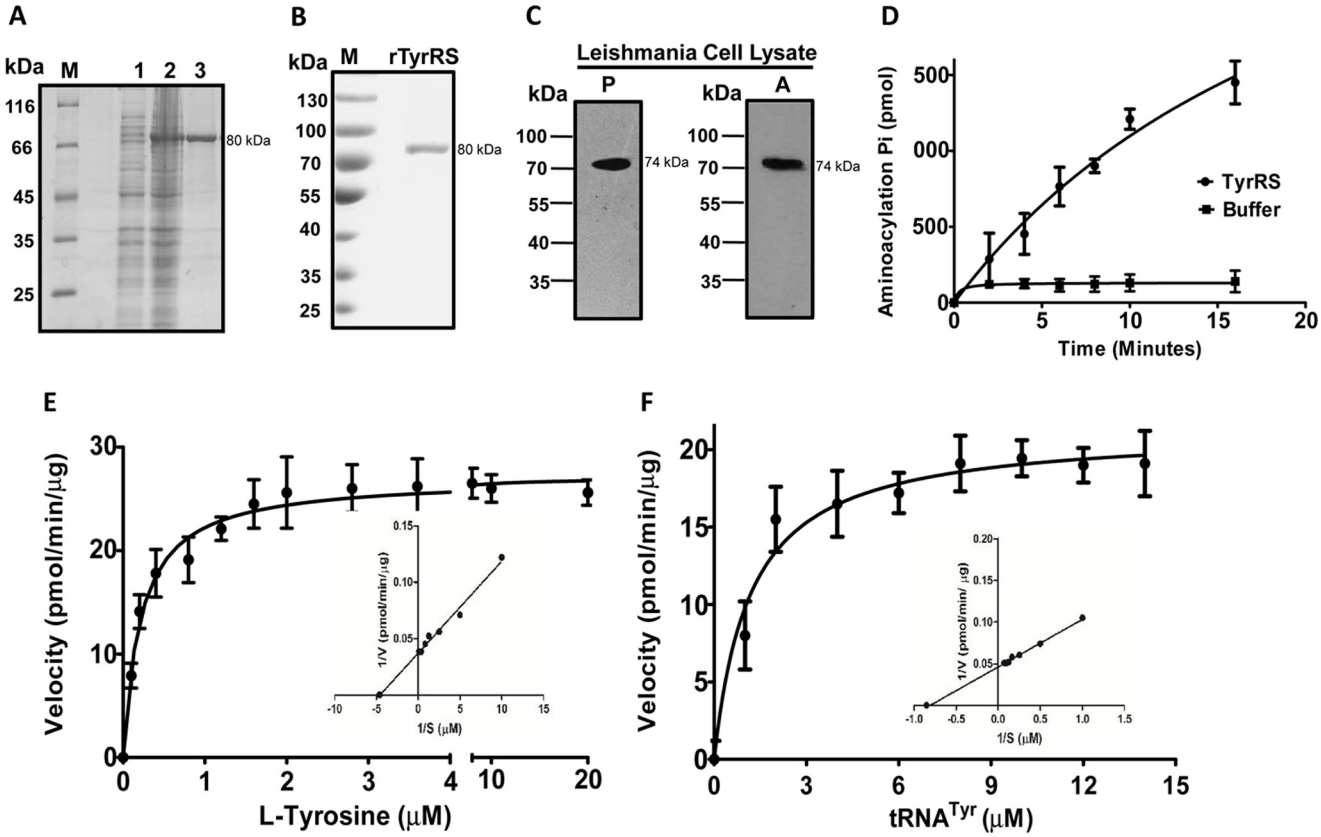

FIGURE 3. **Purification and enzymatic characterization of recombinant *Ld*TyrRS.** *A,* purification of recombinant *Ld*TyrRS protein on nickel-nitrilotriacetic acid affinity resin. *M*, molecular weight marker; *Lane 1*, uninduced cell lysate; *lane 2*, induced cell lysate; *lane 3*, r*Ld*TyrRS. *B,* Western blotting analysis of the recombinant *Ld*TyrRS protein using anti-His tag mouse antibody (1:3000). *rTyrRS*, purified r*Ld*TyrRS. *C,* immunoblotting analysis of the *Leishmania* promastigote (*P*) and amastigote (*A*) cell lysate (~40 μg) with the anti-*Ld*TyrRS antibody. *D,* time course of $tRNA^{Tyr}$ aminoacylation by recombinant *Ld*TyrRS. Reactions were performed with L-tyrosine and $tRNA^{Tyr}$ as the substrates. The data shows an average of three experiments performed in duplicate ± S.D. *E* and *F,* aminoacylation kinetics of *Ld*TyrRS as a function of L-tyrosine concentration (*E*) or $tRNA^{Tyr}$ concentration (*F*). The results represent mean ± S.D. with $n = 3$.

Gene Deletion Studies of Tyrosyl-tRNA Synthetase—Because TyrRS is an important component of protein translation, we explored whether its depletion from the cell would affect aminoacylation and impact parasite growth and infection. The essentiality of *LdTyrRS* was assessed by classical gene replacement experiments where attempts were made to replace both the alleles of *LdTyrRS* by drug-resistance genes. This was achieved by the generation of inactivation cassettes with hygro-

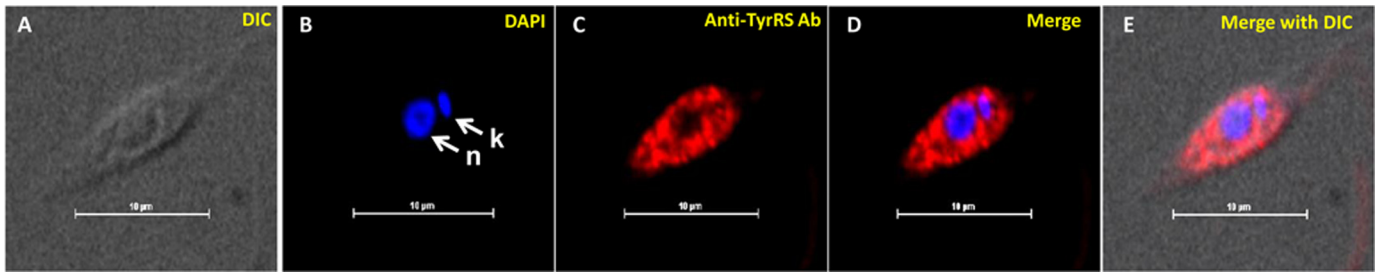

FIGURE 4. **Subcellular localization of *Ld*TyrRS in *L. donovani*.** Immunofluorescence analysis by confocal micrograph of wild-type log phase promastigotes. *Panel A,* phase-contrast image. *Panel B,* promastigotes stained with DAPI. *Panel C,* anti-*Ld*TyrRS antibody detected using Alexa 542 (*red*)-conjugated secondary antibody. *Panels D* and *E,* merged micrographs. *k* and *n* indicate kinetoplastid and nuclear DNA, respectively. The *scale bar* represents 10 μm.

mycin phosphotransferase (*HYG*) or neomycin phosphotransferase (*NEO*) as selection markers along with 5′- and 3′-UTRs of the *TyrRS* gene, as described under "Experimental Procedures." Linear replacement cassettes made by fusion PCR were electrotransfected into wild-type (WT) *L. donovani* promastigotes leading to the generation of heterozygous parasites (*TyrRS*/*HYG* or *TyrRS*/*NEO*) in which one allele of the *LdTyrRS* gene was replaced with either the hygromycin or neomycin drug resistance gene. The replacement of a single allele of the *LdTyrRS* gene by the drug resistance gene cassette was confirmed by a PCR-based analysis. After 3–4 passages, DNA from heterozygous mutant parasites (*TyrRS*/*HYG* or *TyrRS*/*NEO*) was isolated and subjected to a PCR-based analysis using primers external to the inactivation cassette of the *LdTyrRS* gene (Fig. 5*A*). The PCR analysis demonstrated the correct integration of *HYG* and *NEO* replacement cassettes at the *TyrRS* locus in heterozygotes (*TyrRS*/*HYG* or *TyrRS*/*NEO*), as indicated by the appearance of 1.2- (Fig. 5*B*, *lane 1*) and 1.3-kb (Fig. 5*B*, *lane 2*) bands in the case of *HYG* cassette and 1.1- (Fig. 5*B*, *lane 1*) and 1.3-kb (Fig. 5*B*, *lane 2*) bands in the case of *NEO* cassette, along with the 1.0- (Fig. 5*B*, *lane 3*) and 1.3-kb (Fig. 5*B*, *lane 4*) bands corresponding to the WT *LdTyrRS* gene. This data confirmed that a single allele of the *LdTyrRS* gene had been replaced in heterozygous mutant parasites (*TyrRS*/*HYG* or *TyrRS*/*NEO*). Several attempts to replace both alleles of the *LdTyrRS* gene to generate homozygous gene deletion mutants failed. Although few clones resistant to both drugs were obtained, PCR analyses demonstrated that the *LdTyrRS* gene was still present in the genome of these parasite lines (data not shown), thus indicating that *LdTyrRS* is an essential gene.

The effect of disruption of a single allele of the *TyrRS* gene at the protein level was studied by Western blotting analysis. Densitometric analysis was performed to evaluate the levels of TyrRS protein across different parasite lines. Comparative densitometry of the bands revealed a ~1.8-fold decreased expression of *TyrRS* protein in heterozygous mutants (*TyrRS*/*HYG*) (Fig. 5*C*, *lane 4*) as compared with that in WT parasites. Complementation of the heterozygous mutant parasites (*TyrRS*/*HYG*) with an episomal copy of the *TyrRS* gene (*TyrRS*/*HYG*-*[pTyrRS*$^+$*]*) restored protein expression to levels comparable with that of WT parasites (Fig. 5*C*, *lane 3*). The overexpression of *Ld*TyrRS protein in overexpressing mutants (*WT[pTyrRS*$^+$*]*) was also confirmed by Western blotting analysis. A ~1.5-fold increase in the *TyrRS* protein level was observed in *TyrRS* overexpressors (*WT[pTyrRS*$^+$*]*) (Fig. 5*C*, *lane 1*) as compared with that in WT parasites.

To further establish that the elimination of a single allele of the *TyrRS* gene in *L. donovani* conferred *TyrRS* enzyme deficiency, the aminoacylation activity of TyrRS was determined in genetically manipulated parasites and compared with that in WT *L. donovani* parasites. A ~2-fold decrease in the aminoacylation activity of TyrRS was observed in heterozygous parasites (*TyrRS*/*HYG*) as compared with that in WT parasites (Fig. 5*D*). Similar results were obtained with *TyrRS*/*NEO* parasites (data not shown). The WT and the "add-back" lines (*TyrRS*/*HYG[pTyrRS*$^+$*]*) exhibited comparable TyrRS activity levels (Fig. 5*D*).

To assess if the reduced expression of TyrRS compromised the cellular growth of heterozygous mutant parasites, growth kinetic studies were undertaken. Heterozygous parasites (*TyrRS*/*HYG*) consistently showed growth delay as compared with WT parasites (Fig. 5*E*). The complementation of *TyrRS*/*HYG* mutants with an episomal copy (*pTyrRS*$^+$) rescued the growth of these parasites similar to that of the WT control. Thus, it is reasonable to assume that a gene dosage effect resulted in the production of lesser *TyrRS* protein, and such a conjecture would suggest that *TyrRS* is involved in optimal cell proliferation.

We also examined the survival of heterozygous mutant parasites (*TyrRS*/*HYG*) inside murine macrophages *in vitro*. Virulence studies in a mouse macrophage cell line were carried out to determine the effects of genetic deficiency of *TyrRS* and to characterize the *Ld*TyrRS enzyme further as a potential therapeutic target. To this end, a murine macrophage cell line was infected with WT, *TyrRS* heterozygous mutant (*TyrRS*/*HYG*), and add-back (*TyrRS*/*HYG[pTyrRS*+*]*) parasites at an multiplicity of infection of 20:1. WT parasites were capable of infecting and sustaining robust infection in murine macrophages, whereas the parasitemia of the heterozygous mutants was reduced by ~50% relative to WT parasites 24 h post-infection (Fig. 5*F*). Similar results were obtained with *TyrRS*/*NEO* parasites (data not shown). Complementation with an episomal copy of the *TyrRS* gene restored the infectivity of the heterozygous (*TyrRS*/*HYG*) mutants similar to that of the WT parasites. Taken together, our data suggests that the *LdTyrRS* gene has a significant role in the growth and intramacrophage survival of amastigotes.

Leishmanicidal Activity of TyrRS Inhibitors—Resveratrol is a natural phenolic compound that has recently been shown to inhibit the activity of human TyrRS (19). A co-crystal structure of resveratrol bound to the active site of human TyrRS has been reported (19). Another flavanoid compound fisetin has also been identified to bind TyrRS of *L. major* (13). To test the effi-

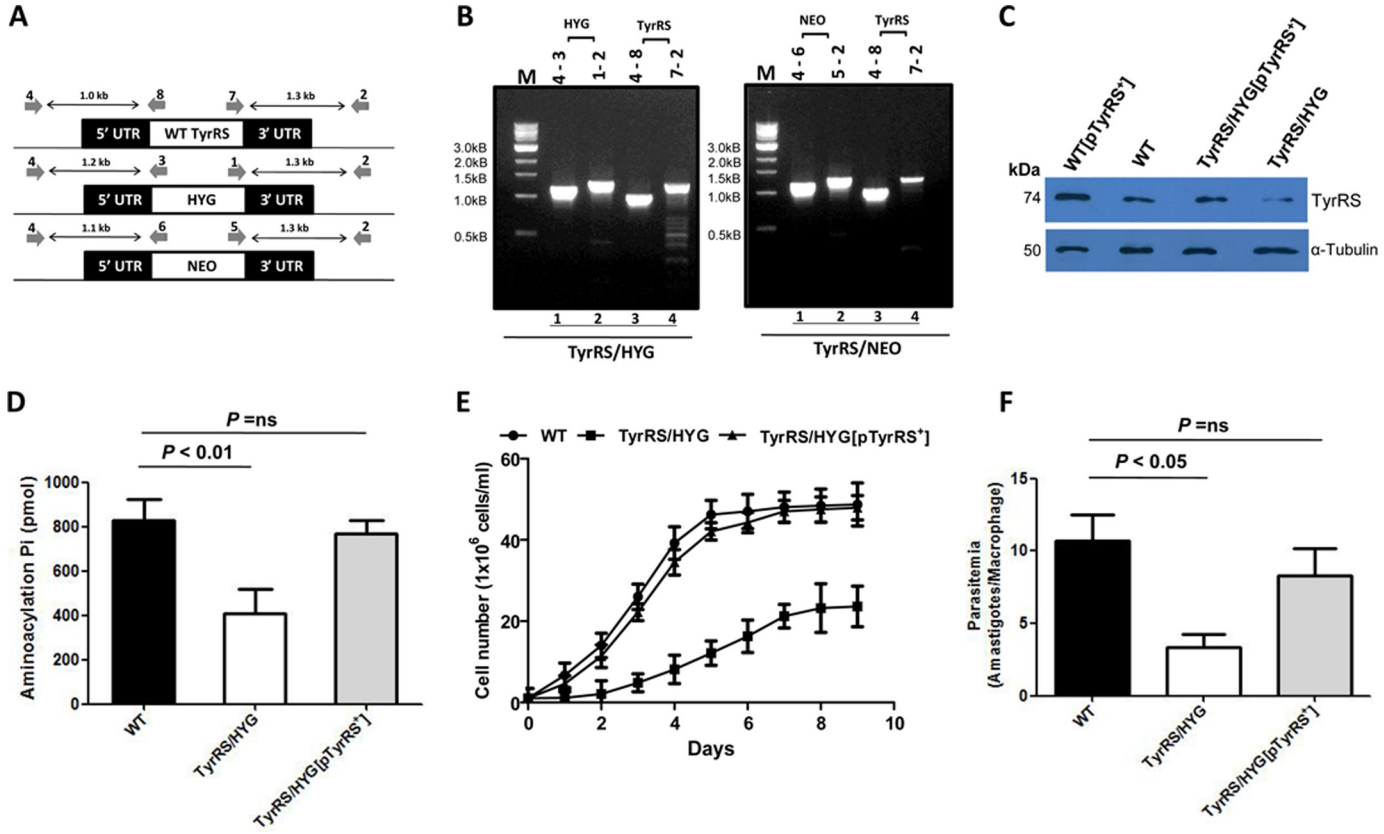

FIGURE 5. **Generation and characterization of heterozygous knock-out mutants of *LdTyrRS*.** *A,* map of *LdTyrRS* genomic locus and location of the primers used for confirmation by PCR-based analysis along with the expected band sizes. Primer 4 was designed as a forward primer to match the upstream region of the *LdTyrRS* gene, and primers 8, 3, and 6 were designed internal to *TyrRS, HYG,* and *NEO* coding regions, respectively. Primer 2 was designed as a reverse primer to match the downstream region of *LdTyrRS* gene, and primers 7, 1, and 5 were designed as forward primers, internal to *TyrRS, HYG,* and *NEO* coding regions, respectively. *B,* genomic DNA from heterozygous *TyrRS/HYG* and *TyrRS/NEO* mutant parasites was used as a template for PCR analysis. The specific integration of the replacement cassette was checked with *HYG*, *NEO*, and *LdTyrRS* (WT) gene-specific primers. *M* indicates the molecular size marker in kb. *C,* Western blotting analysis of equal protein quantities (~30 μg) from whole cell lysates prepared from WT, *TyrRS* overexpressors (*WT[pTyrRS$^+$]*), add-back (*TyrRS/HYG[pTyrRS$^+$]*), and heterozygous mutant (*TyrRS/HYG*) parasites. The loading was normalized with α-tubulin (50 kDa) antibody. *D,* comparison of the aminoacylation activity of TyrRS in cell lysate of WT, heterozygous (*TyrRS/HYG*) mutant, and add-back (*TyrRS/HYG*[*pTyrRS*$^+$]) parasites. *E,* growth curve of *L. donovani* WT, add-back (*TyrRS/HYG*[*pTyrRS*$^+$]), and heterozygous mutant (*TyrRS/HYG*) promastigotes in M199 media. The results represent mean ± S.D. with $n = 3$. *F,* comparison of infectivity of *L. donovani* WT, heterozygous mutant (*TyrRS/HYG*), and add-back (*TyrRS/HYG*[p*TyrRS*$^+$]) parasites in J774A.1 murine macrophage cell line. The murine macrophage cell line J774A.1 was infected with the stationary-phase promastigotes at an multiplicity of infection of 20:1. The cells were stained after 24 h and amastigotes enumerated visually. The results represent mean ± S.D. with $n = 3$. Student's *t* test was performed, and the *p* values are indicated.

cacy of these compounds on *L. donovani*, log phase promastigotes were cultured in the presence of increasing concentrations of fisetin and resveratrol. Both compounds were found to inhibit the growth of promastigotes in a dose-dependent manner (Fig. 6*A*). The effective concentration that caused 50% inhibition of growth (IC_{50}) after 72 h of drug addition was 31.07 μM for fisetin and 47.21 μM for resveratrol (Fig. 6*A*). The sensitivities of amastigotes were also tested in an intracellular amastigote-macrophage model. The IC_{50} of fisetin and resveratrol for amastigotes after 3 days of drug treatment was 1.53 and 9.3 μM, respectively (Fig. 6*B*). At these concentrations, both fisetin and resveratrol did not affect the viability of the macrophage cell line J774A.1, with the IC_{50} being >400 μM after 48 h of drug treatment.

The effect of these compounds on the aminoacylation activity of *Ld*TyrRS (Fig. 6*C*) was also tested. Fisetin inhibited the enzymatic activity of recombinant *Ld*TyrRS with an IC_{50} of ~14.23 μM (Fig. 6*C*), whereas a concentration of resveratrol as high as 1 mM failed to inhibit the enzymatic activity of *Ld*TyrRS (Fig. 6*C*). Thus, our results suggest that the anti-leishmanial effect of resveratrol is not due to the inhibition of *Ld*TyrRS.

To ascertain whether the anti-leishmanial activity of fisetin is mediated through the inhibition of *Ld*TyrRS, we also evaluated the effect of fisetin on the growth of genetically manipulated parasites (Fig. 6*D*). WT, overexpressors (*WT[pTyrRS$^+$]*), heterozygous mutants (*TyrRS/HYG*), and add-back (*TyrRS/HYG[pTyrRS$^+$]*) parasites were treated with fisetin at a concentration of 35 μM. In the absence of drug treatment (untreated), the growth of each parasitic line was normalized to a value of 1.0. After 72 h of treatment with fisetin, the growth rate of each parasitic line was calculated relative to the untreated control. Parasites overexpressing *Ld*TyrRS (*WT[pTyrRS$^+$]*) were found to be more resistant to growth inhibition by fisetin as compared with WT parasites (Fig. 6*D*). In contrast, heterozygous mutant parasites (*TyrRS*/*HYG*) were found to be more susceptible to inhibition by fisetin when compared with WT parasites (Fig. 6*D*). Complementation of *TyrRS*/*HYG* parasites with an episomal *TyrRS* gene (*TyrRS*/*HYG[pTyrRS$^+$]*) decreased the sen-

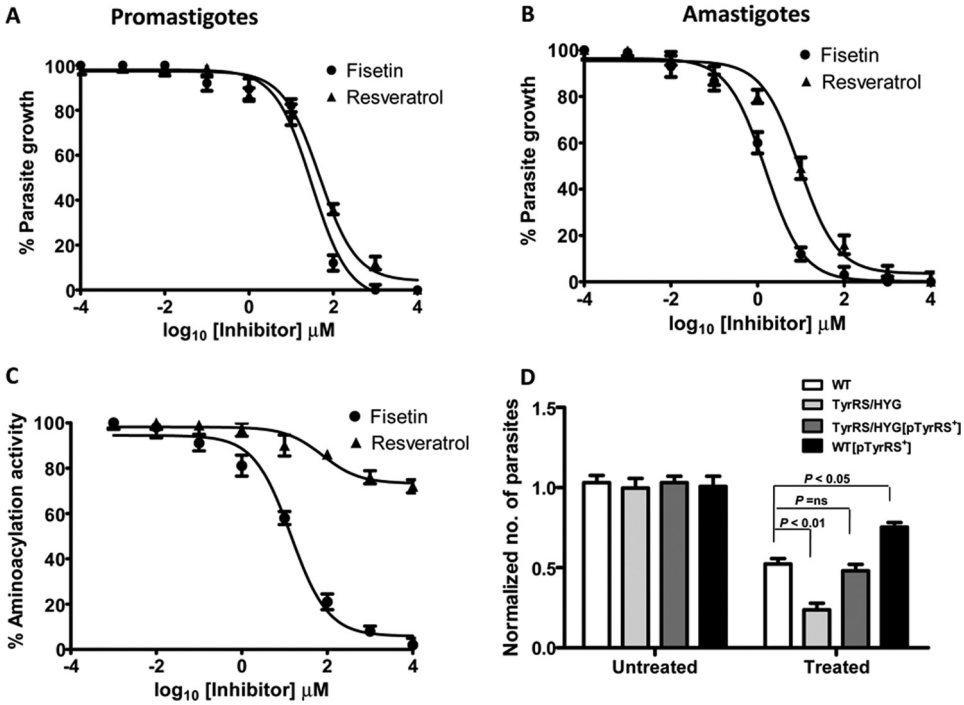

FIGURE 6. **Effect of TyrRS inhibitors on parasite growth and enzyme activity.** *A,* inhibition of promastigote growth in the presence of resveratrol and fisetin. The assay was done in 96-well plates and growth was estimated by 3-(4,5-dimethylthiazol-2-yl)-2,5-diphenyltetrazolium bromide assay. Percentage growth of parasite was plotted against different concentrations of inhibitors. *B,* effect of resveratrol and fisetin on amastigote growth progression was studied by observing Giemsa-stained infected macrophages under a microscope. *C,* inhibition of r*Ld*TyrRS aminoacylation activity by resveratrol and fisetin. *D,* comparison of the effect of fisetin activity on WT and genetically manipulated parasites. WT, overexpressors (*WT[pTyrRS*$^+$*]*), heterozygous mutants (*TyrRS*/HYG), and add-back (*TyrRS/HYG[TyrRS*$^+$*]*) parasites were treated with fisetin at a concentration of 35 μM. The cell growth was determined after 72 h. In the absence of drug treatment (untreated), the growth of each parasitic line was normalized to 1.0. After treatment with fisetin (*treated*), growth was calculated relative to the corresponding untreated control. The bar graph represents the mean ± S.D. with $n = 3$. Student's *t* test was performed, and *p* values are indicated.

sitivity of heterozygous mutant parasites (Fig. 6*D*). The increased susceptibility of the heterozygous mutants to fisetin may be explained by the reduced levels of *Ld*TyrRS expression in heterozygous knock-out parasites. The above data further indicates that fisetin exerts its antileishmanial effect through the inhibition of *Ld*TyrRS.

Localization of TyrRS during Macrophage Infection with Leishmania—To determine the localization of *Ld*TyrRS during macrophage infection, confocal microscopy of infected macrophages was performed. Infected and uninfected macrophages were fixed, permeabilized, and processed for immunofluorescence using either the anti-*Ld*TyrRS antibody or preimmune sera (Fig. 7, *B* and *C*). DAPI staining was utilized for visualizing both the host and parasite nuclei. The anti-*Ld*TyrRS-specific fluorescence observed in infected macrophages was not only associated with parasite nuclei staining but was also present throughout the cytosol of the infected macrophages (Fig. 7*C*). Thus, the confocal data demonstrates the presence of *Ld*TyrRS in the cytosol of infected macrophages. Uninfected macrophages served as a negative control (Fig. 7*A*). No signal could be detected with the preimmune sera in infected macrophages (Fig. 7*B*). The immunofluorescence data thus indicates the possible secretion of TyrRS from *Leishmania* amastigotes (Fig. 7, *A*–*C*).

The presence of *Ld*TyrRS in the host cytosol also hinted toward its possible secretion into the extracellular milieu. Therefore, culture supernatants from uninfected or *L. donovani*-infected macrophages were analyzed for the presence of *Ld*TyrRS by immunoprecipitation and immunoblotting analysis (Fig. 7*D*). As expected, no TyrRS was detected in the culture supernatant of uninfected macrophages (Fig. 7*D*). In contrast, a single band corresponding to the wild-type *Ld*TyrRS (~74 kDa) was observed in the culture supernatant of infected macrophages (Fig. 7*D*).

We also analyzed the secretion of TyrRS by *Leishmania* promastigotes (Fig. 7*E*). A ~74-kDa band corresponding to wild-type *Ld*TyrRS was observed in the parasite culture supernatants (Fig. 7*E*). To exclude the possibility that the apparent secretion of *Ld*TyrRS was due to cell lysis, we measured the amount of the cytosolic marker glucose-6-phosphate dehydrogenase in the parasite (promastigote) culture supernatants by an enzymatic assay (20). The glucose-6-phosphate dehydrogenase activity in culture supernatants was found to be negligible (data not shown). As a control, parasite culture supernatants were also analyzed for the presence of mitochondrial tryparedoxin peroxidase, which has been reported to be a parasitic non-secretory protein (21) (Fig. 7*F*). No secretion of mitochondrial tryparedoxin peroxidase was observed in promastigote culture supernatants (Fig. 7*F*). Taken together, our immunofluorescence, immunoprecipitation, and Western blotting data provide compelling evidence indicating the secretion of *Ld*TyrRS from both promastigotes and amastigotes.

Tyrosyl-tRNA Synthetase of Leishmania Possesses an Immunologically Active ELR Motif —Previously, human "mini"-TyrRS has been shown to display potent neutrophil chemotaxis activity because of the presence of an immunologically active

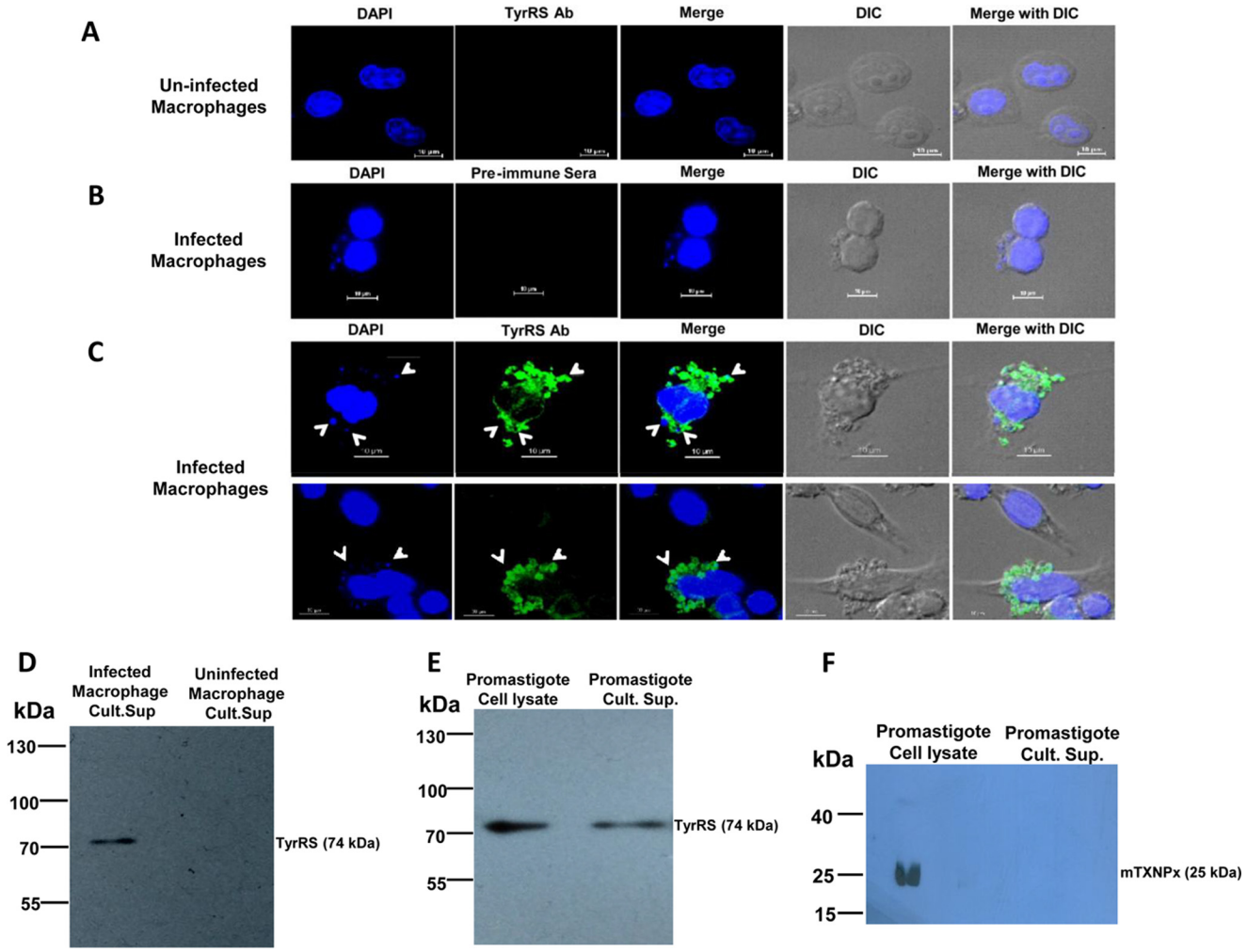

FIGURE 7. **Localization of the *Ld*TyrRS in infected macrophages.** *A–C*, confocal microscopy of the uninfected (*A*) and *L. donovani*-infected macrophages (*B* and *C*) showing the secretion of *Ld*TyrRS protein in the macrophage cytoplasm. *White arrows* indicate intracellular amastigotes. Parasite and macrophage nuclei were visualized with DAPI (*blue*). Anti-*Ld*TyrRS antibody (*green*) was used to visualize the parasitic *Ld*TyrRS. Staining of infected macrophages with rabbit preimmune sera was used as a negative control (*B*). *Scale bar* corresponds to a size of 10 μm. *D,* Western blotting analysis of the parasite culture supernatants using antibodies against *Ld*TyrRS. The culture supernatant of the infected (*lane 1*) and uninfected (*lane 2*) macrophages was electroblotted onto nitrocellulose membrane and probed with the anti-*Ld*TyrRS antibody and HRP-conjugated anti-rabbit antibody. The blot was then developed with commercially available ECL reagent. Western blotting analysis of the promastigote culture supernatants was used to check for the presence of *Ld*TyrRS (*E*) and mitochondrial tryparedoxin peroxidase (*mTXNPx*) (*F*). *Lane 1*, *L. donovani* promastigote cell lysate (20 μg); *lane 2,* promastigote culture supernatant. The parasites were suspended at a concentration of $\sim 10^8$ parasites/ml in RPMI 1640 media without FBS and incubated for 8 h under normal culture conditions. The *Ld*TyrRS protein was immunoprecipitated from a minimum of ~80 ml of culture supernatants containing a total of $\sim 8 \times 10^9$ promastigotes and detected by a Western blotting analysis as described under "Experimental Procedures."

ELR motif (4). A transwell migration assay was performed to evaluate the chemotactic activity of *Ld*TyrRS toward mouse neutrophils (Fig. 8*A*). The neutrophils that migrated into the lower chamber were quantitated by measuring their myeloperoxidase activity (Fig. 8*B*) as described under "Experimental Procedures." *N*-Formyl-Met-Leu-Phe (fMLP) is a chemotactic peptide that was used as a positive control. The addition of both fMLP and r*Ld*TyrRS stimulated the chemotactic migration of neutrophils (Fig. 8, *B* and *C*). Recombinant *Ld*TyrRS stimulated the chemotactic activity of neutrophils at a concentration of 0.1 nM (6 ng), which is equivalent to the physiological amount of protein present in $\sim 2 \times 10^5$ parasites. Because the ELR motif is critical for chemotactic activity, we also prepared *Ld*TyrRS mutant in which the ELR motif was mutated to "AAA." The mutant *Ld*TyrRS (ELR/AAA) did not show any chemotactic activity toward neutrophils (Fig. 8, *B* and *C*). Also, under these experimental conditions, spontaneous migration of neutrophils was negligible as indicated by the media control (Fig. 8, *B* and *C*).

Overall, these results suggest that because of its ELR motif, *Ld*TyrRS functions as a chemoattractant for neutrophils. It is also known that the *Leishmania* parasite exploits neutrophils as Trojan horses before they enter their definitive host cells, *i.e.* macrophages (22). In light of the role of neutrophils as host cells for *Leishmania*, it may be hypothesized that secreted *Ld*TyrRS functions as a virulence factor to induce an inflammatory recruitment of neutrophils at the site of infection.

LdTyrRS Interaction with Host Macrophages—In addition to attracting neutrophils, another important function of the ELR motif is to mediate the interaction of CXC chemokines with host immune cells like macrophages. This interaction further triggers the release of proinflammatory cytokines from host

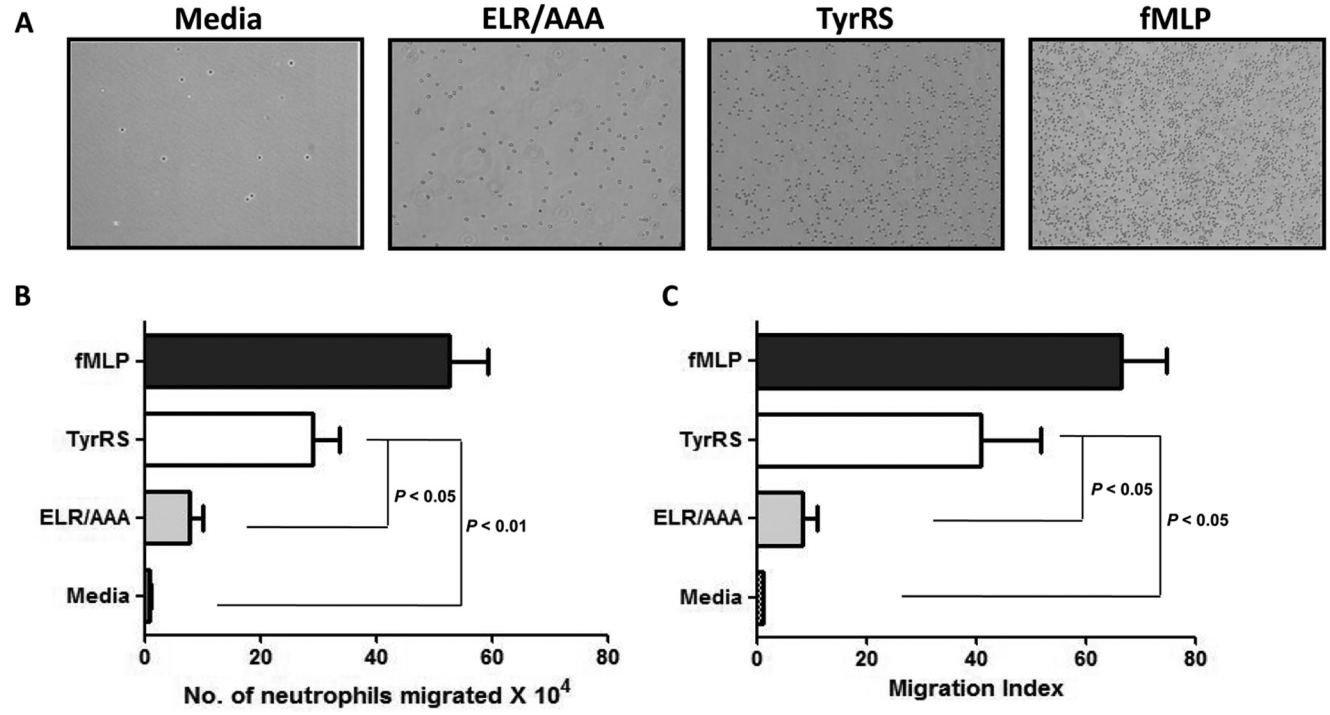

FIGURE 8. **The effect of *Ld*TyrRS on neutrophil chemotaxis was studied by a transwell assay.** Wild-type r*Ld*TyrRS, mutated r*Ld*TyrRS (ELR/AAA), media (negative control), and fMLP (positive control) were used as chemoattractants. *A* shows a representative photograph of the cell migration in each condition. *B,* the number of cells that migrated due to the effect of different chemoattractants were quantitated using a myeloperoxidase assay. *C,* migration is also plotted as migration index (the number of cells migrating in each condition/number of cells migrating in basal medium). Data (*i.e.* the number of neutrophils migrated and the migration index) are represented as mean ± S.D. with $n = 4$. Student's *t* test was performed, and *p* values are indicated.

immune cells (23–25). Direct binding of r*Ld*TyrRS to host macrophages was visualized by immunofluorescence analysis. The specific interaction of r*Ld*TyrRS with mouse macrophages was observed by using anti-*Ld*TyrRS (Fig. 9*A*) and anti-His antibodies (Fig. 9*E*). On the other hand, the mutant *Ld*TyrRS (ELR/AAA) did not show any binding to host macrophages (Fig. 9, *B* and *F*). Also, no binding could be detected in macrophages that were not incubated with any protein and preimmune sera controls (Fig. 9, *C* and *D*). This data indicated an ELR motif-mediated interaction of *Ld*TyrRS with host macrophages.

Triggering of Cytokine Secretion by LdTyrRS—To check if *Ld*TyrRS triggers cytokine activity, a murine macrophage cell line was incubated with r*Ld*TyrRS, mutant ELR/AAA-*Ld*TyrRS, lipopolysaccharide (LPS) (as a positive control), and r*Ld*LeuRS (as a negative control). The culture supernatants were analyzed for the presence of proinflammatory cytokines such as TNF-α, IL-6, IL-12, and IFN-γ. Time kinetic analysis by ELISA revealed maximal production of the inflammatory cytokine TNF-α (Fig. 10*A*) during 12 h of culture and IL-6 within 24 h of culture (Fig. 10*B*). Interestingly, the mutant ELR/AAA-*Ld*TyrRS did not trigger cytokine release from macrophages and behaved similarly to the control protein r*Ld*LeuRS (Fig. 10, *A* and *B*). Moreover, the release of TNF-α and IL-6 by r*Ld*TyrRS was mediated in a concentration-dependent manner (Fig. 10, *C* and *D*). Other proinflammatory cytokines like IL-12 and IFN-γ were not induced by r*Ld*TyrRS (Fig. 10*E*). We also checked the induction of an important anti-inflammatory cytokine, IL-10, which is involved in disease progression in leishmaniasis (26). Recombinant *Ld*TyrRS failed to trigger IL-10 secretion (Fig. 10*E*) by host macrophages. This data indicates that *Ld*TyrRS specifically triggers the release of IL-6 and TNF-α in a time- and dose-dependent manner.

We also corroborated our findings with the native *Ld*TyrRS that was immunoprecipitated from promastigote culture supernatants (PDTyrRS). Native *Ld*TyrRS was equally capable of triggering TNF-α and IL-6 release from murine macrophages (Fig. 11, *A* and *B*). It was also observed that preincubation of native *Ld*TyrRS (PDTyrRS) with anti-*Ld*TyrRS antibodies (PDTyrRS + αTyrRS) substantially blocked TNF-α ($p < 0.001$) and IL-6 production ($p < 0.001$) from macrophages (Fig. 11, *A* and *B*), thereby suggesting a specific motif-based *Ld*TyrRS interaction with host macrophages.

Potential Receptor(s) of LdTyrRS on Host Macrophages—ELR motif-based binding of CXC chemokines to a CXCR2 receptor on immune cells has been shown to activate NF-κB and induce proinflammatory cytokine expression (23). To determine whether the binding of *Ld*TyrRS is also mediated through ELR-CXCR2 receptor interaction, we preincubated human macrophages with anti-CXCR2 and anti-*Ld*TyrRS antibodies and tested whether antibody-mediated receptor or protein blockades inhibited r*Ld*TyrRS-macrophage interaction. The interaction was analyzed by FACS analysis. Recombinant *Ld*TyrRS bound to mouse macrophages was detected by an anti-*Ld*TyrRS antibody (Fig. 12*A*). On the other hand, specific antibody-mediated blocking of the CXCR2 receptor on murine macrophages reduced r*Ld*TyrRS binding (Fig. 12*B*). The blocking of r*Ld*TyrRS protein with anti-*Ld*TyrRS antibodies also reduced binding of the protein to macrophages (Fig. 12*C*). As expected, mutant *Ld*TyrRS (ELR/AAA) protein did not show

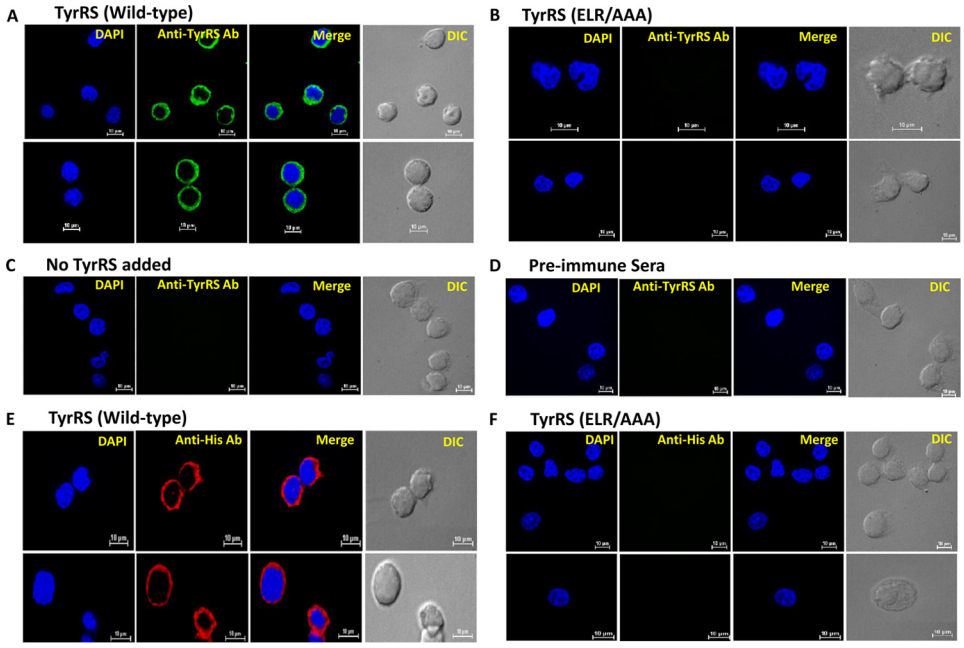

FIGURE 9. ***Ld*TyrRS interaction with macrophages *in vitro*.** *A* and *B,* confocal images representing the binding of r*Ld*TyrRS (*green*) (*A*) and mutant *Ld*TyrRS (ELR/AAA) to mouse macrophages (*B*). *C* and *D,* represent controls for primary/secondary antibodies alone (that is, no added *Ld*TyrRS) (*C*) and preimmune sera (*D*). For nucleus visualization, DAPI (*blue*) localization is shown. The interaction of *Ld*TyrRS with the mouse macrophage cell line was visualized by staining with the anti-*Ld*TyrRS antibody (*A–D*). *E* and *F*, the binding of r*Ld*TyrRS (*E*) and ELR/AAA mutant *Ld*TyrRS (*F*) to mouse macrophages was also detected using anti-His monoclonal antibody. The *scale bar* corresponds to a size of 10 μm.

any binding to host macrophages (Fig. 12*D*). Furthermore, blockage of r*Ld*TyrRS-macrophage interactions using either anti-CXCR2 or anti-*Ld*TyrRS antibodies significantly reduced the release of TNF-α ($p < 0.001$) and IL-6 ($p < 0.001$) from murine macrophages (Fig. 12, *E* and *F*). Our data strongly highlights the role of ELR motif in mediating *Ld*TyrRS interactions with host macrophages. We, therefore, conclude that ELR motif-based *Ld*TyrRS binding *in vitro* likely occurs using specific receptors on host macrophages and that this binding might lead to very specific host immune system activation.

Discussion

aaRSs are key enzymes that drive the protein translational machinery. Apart from their translational functions, aaRSs are implicated in various non-canonical functions such as gene transcription, mRNA translation, inflammation, and immune response (1). Therefore, aaRSs constitute a significant subset of proteins, and inhibition of their enzymatic activity can be deleterious to the organism. Hence, experimental dissection of critical translation components like aaRSs is on high priority as one of the avenues of novel target discovery in pathogen biology.

TyrRS are yet to be experimentally investigated as drug targets in parasites. The few parasite-specific studies available on TyrRS have majorly focused on the structural aspects of the enzyme. A recent comprehensive study highlighted the structural and functional aspect of TyrRS from *Plasmodium falciparum* (24). The structural analysis of the TyrRS orthologue from *L. major* reveals several crucial differences between the host and pathogen tyrosyl-tRNA synthetase active sites (13). These differences could potentially be exploited for the design of structure-based inhibitors of parasite TyrRSs. The present study highlights the functional attributes of tyrosyl-tRNA synthetase of *Leishmania* as a housekeeping protein translation enzyme and also as a mimic of host CXC chemokine.

In the present study, we, for the first time, report the characterization of tyrosyl-tRNA synthetase from *L. donovani* (*Ld*TyrRS). The overall K_m values deduced by kinetic analysis for *Ld*TyrRS appear to be closer to the K_m values reported for other mammalian TyrRS. *TyrRS* appears to be an essential gene as attempts to delete both copies of the *TyrRS* gene from the parasite genome failed. Heterozygous parasites (*TyrRS*/*HYG*) were found to have slower growth kinetics and exhibited attenuated virulence. Because *L. donovani TyrRS* appears to be an essential gene for parasite survival, we also analyzed the efficacy of known tyrosyl-tRNA synthetase inhibitors, resveratrol and fisetin, on parasite survival and the aminoacylation activity of *Ld*TyrRS. Fisetin was found to inhibit the parasite growth by inhibiting the *Ld*TyrRS aminoacylation activity. This data are in agreement with a previous report that suggests binding of fisetin to the active site of trypanosomal TyrRS (13). Several subtle yet crucial differences between *Leishmania* and human TyrRS (13) could potentially be exploited for the design of structure-based inhibitors for *Ld*TyrRS.

Leishmania has evolved sophisticated mechanisms to evade or subvert host immune responses and establish chronic infection. *Leishmania* parasites have the capacity to subvert phagocytosis (27) and modulate cytokine secretion (11, 28), thus allowing the parasite to thrive within phagocytic cells and within the host organism as a whole. From previous studies, it has become clear that a range of effector molecules secreted by the *Leishmania* parasite play a vital role in this process (20, 29). In this context, the expression of a mimic of a human cytokine

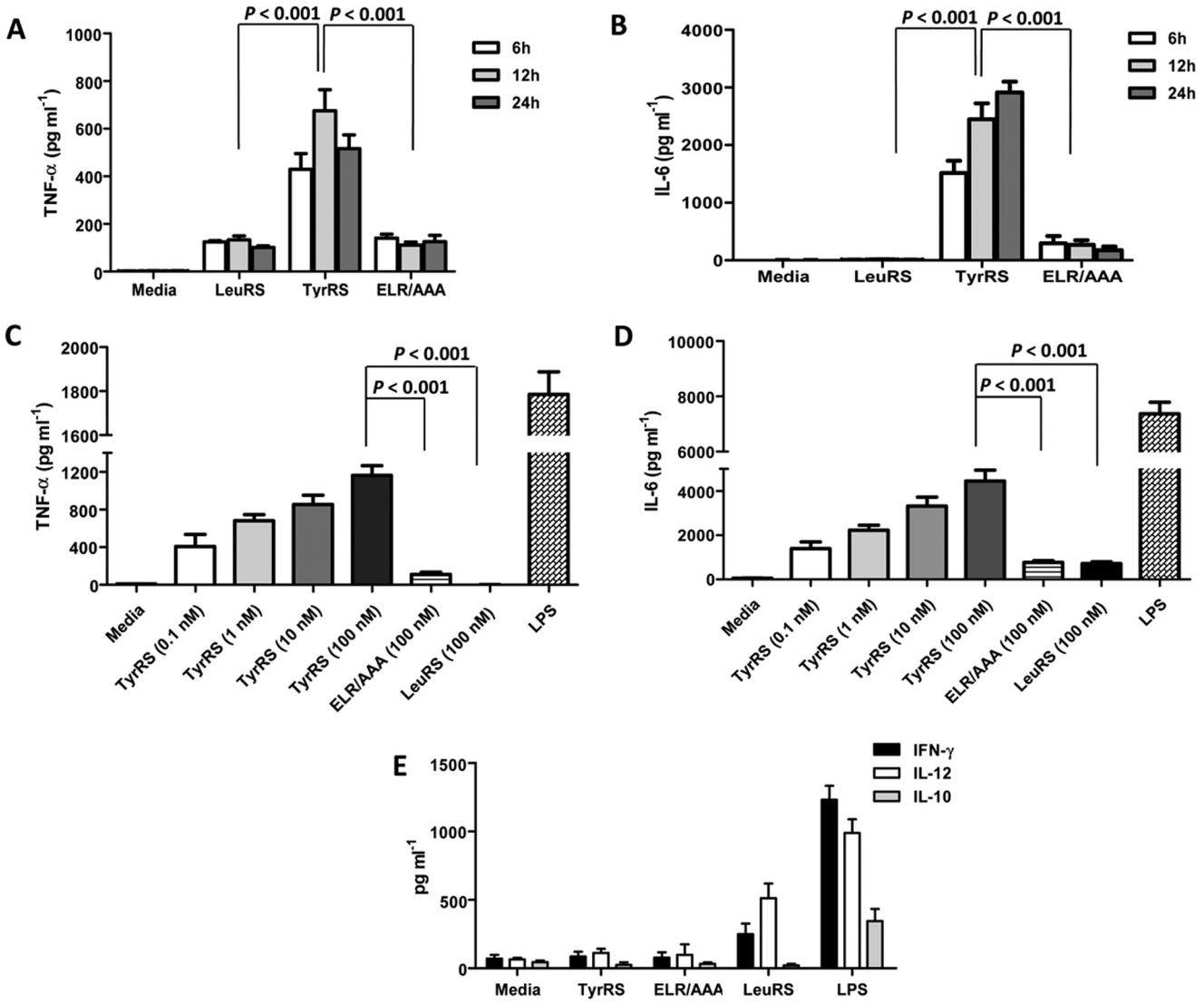

FIGURE 10. **Effect of r*Ld*TyrRS on mouse macrophages.** *A* and *B*, the secretion profile of TNF-α (*A*) and IL-6 (*B*) was measured at different time points using ELISA. *C* and *D*, dose-dependent increase in the secretion of cytokines like TNF-α (*C*) and IL-6 (*D*) from mouse macrophages was also measured. Media alone, r*Ld*LeuRS enzyme, and ELR-AAA mutant of *Ld*TyrRS were used as negative controls. LPS was used as a positive control in all the experiments. *E*, the secretion profile of other cytokines like IFN-γ, IL-10, and IL-12 that are secreted from mouse macrophages on exposure to r*Ld*TyrRS was also analyzed. The results represent mean ± S.D. with $n = 3$. Tukey's test was performed, and p values are indicated.

could contribute to the modulation of host signaling pathways to the advantage of the parasite. This report highlights the moonlighting activity of a parasitic tyrosyl-tRNA synthetase (*Ld*TyrRS) to function as a mimic of host CXC chemokine. Aminoacyl-tRNA synthetases have a vital role in translating the genetic code. Numerous studies have shown that members of this enzyme family are quite adept at "moonlighting" (1, 3, 30). Non-canonical roles have been suggested for several parasite tRNA synthetases. Studies have indicated that human tyrosyl-, tryptophanyl-, and lysyl-tRNA synthetases can be secreted extracellularly and can mimic cytokines (4, 31, 32). TyrRS of *Plasmodium* and LysRS of *Entamoeba* also mimic the functions of human cytokines (24, 33).

Our immunofluorescence and immunoblotting data reveal that both promastigotes and amastigotes secrete *Ld*TyrRS. Interestingly, the secreted tyrosyl-tRNA synthetase from *L. donovani* was found to lack a classical N-terminal secretion signal peptide. Previous reports have identified secretion by exosomes as a major mechanism by which *Leishmania* exports secreted virulence factors that help in communication with the host (29, 34). Due to the absence of any defined secretory signal, it may be hypothesized that the release of *Ld*TyrRS also occurs by a non-classical secretion mechanism. Understanding the exact mechanism by which the secretion of *Ld*TyrRS occurs remains to be explored and is the focus of ongoing work.

We further investigated the capacity of *Ld*TyrRS to modulate neutrophil recruitment. Our data shows that by using its ELR motif, secreted *Ld*TyrRS can induce direct chemotaxis of neutrophils. A recent study has highlighted the role of neutrophils as host cells for *Leishmania* (35–37). Although parasite culture supernatants have been found to have chemotactic activity toward neutrophils (35), parasite-secreted protein(s) that specifically trigger the initial recruitment of neutrophils are poorly understood. The present study identifies *Ld*TyrRS present in the parasite culture supernatant, as a parasite secretory protein having the capacity to modulate neutrophil recruitment. Thus,

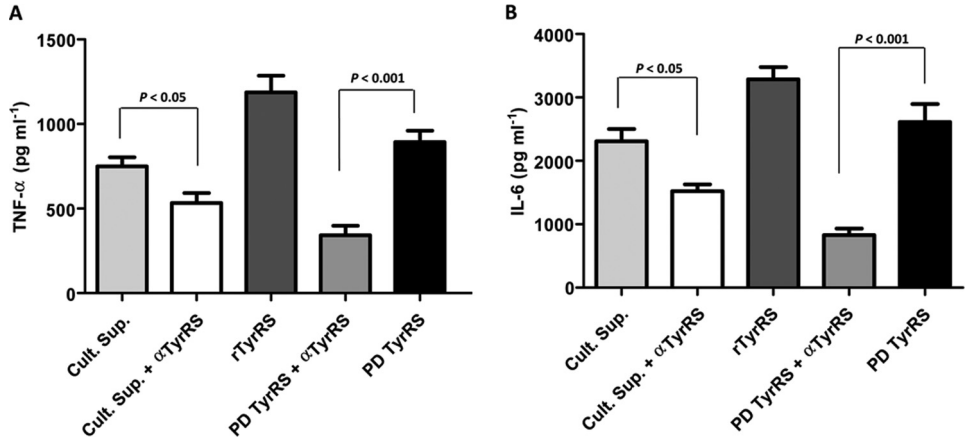

FIGURE 11. **Effect of native *Ld*TyrRS on the cytokine secretion profile of mouse macrophages.** *A* and *B*, secretion profile of TNF-α (*A*) and IL-6 (*B*) using the *L. donovani* promastigote culture supernatants alone (*Cult. Sup.*), promastigote culture supernatants neutralized with the anti-TyrRS antibody (*Sup* + α-*TyrRS Ab*), native *Ld*TyrRS immunoprecipitated from promastigote culture supernatant (*PD-TyrRS*), and finally native *Ld*TyrRS (*PD-TyrRS*) neutralized with its own antibody (*PD-TyrRS* + α-*TyrRS Ab*). Recombinant *Ld*TyrRS was used as a positive control. TNF-α and IL-6 secretion are clearly enhanced significantly when immunoprecipitated native *Ld*TyrRS (*PD-TyrRS*) is used. The triggering activity of native *Ld*TyrRS (*PD-TyrRS* + α-*TyrRS Ab*) is reduced when preincubated with anti-*Ld*TyrRS antibodies (1:3000), indicating specific activation of macrophages with native *Ld*TyrRS (*PD-TyrRS*). The results represent mean ± S.D. with $n = 3$. Tukey's test was performed, and *p* values are indicated.

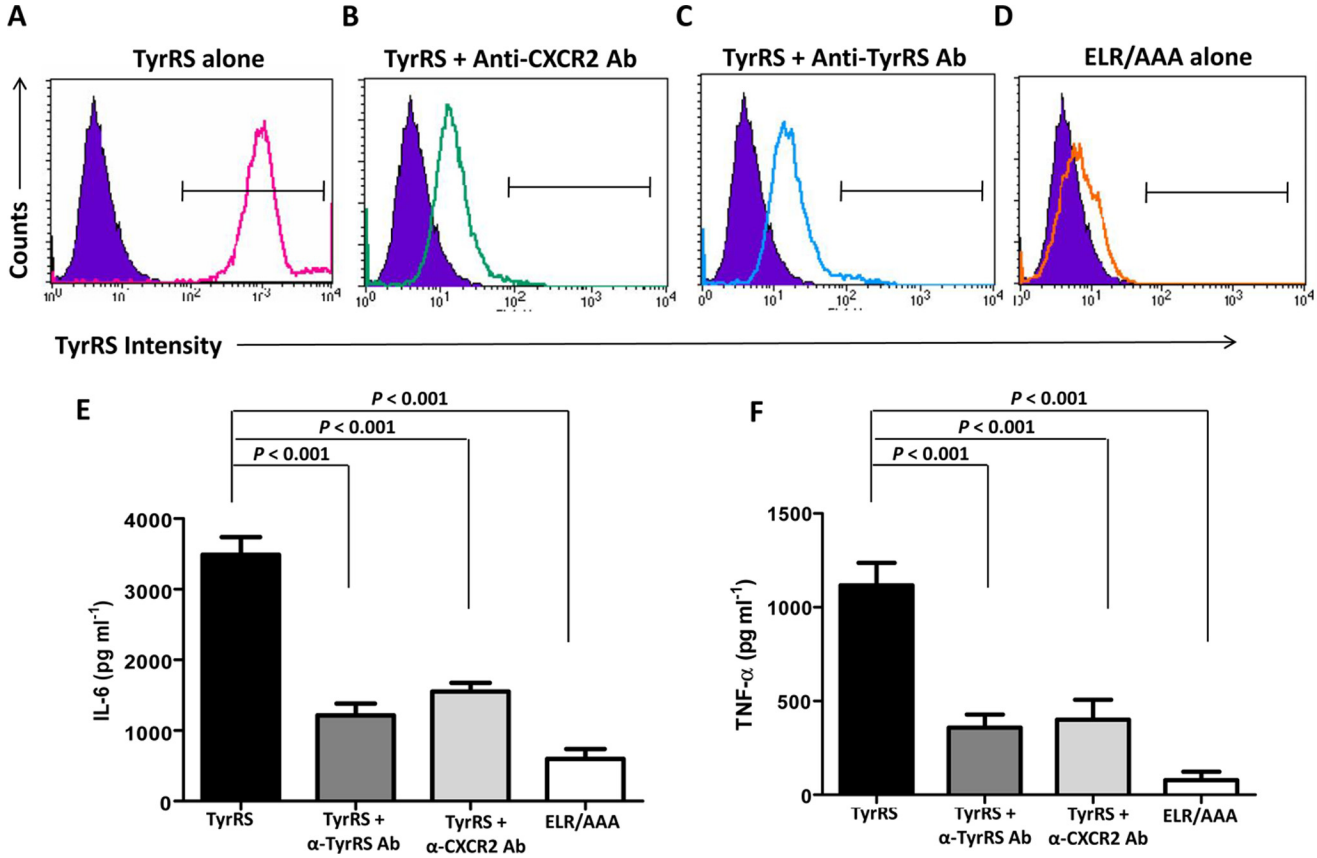

FIGURE 12. **Potential *Ld*TyrRS receptor on mouse macrophages.** *A–D,* FACS analysis to assess the binding of r*Ld*TyrRS to mouse macrophages. r*Ld*TyrRS bound to mouse macrophages was analyzed by indirect staining with the anti-TyrRS antibody. Overlay histograms show binding of r*Ld*TyrRS to the surface of mice macrophages (*solid line*) with unstained controls (*purple solid*) as background. Histogram (*solid line*) shows positive binding of r*Ld*TyrRS to mouse macrophages (*A*). r*Ld*TyrRS binding to macrophages is reduced when macrophages are preincubated anti-CXCR2 (*B*) or when r*Ld*TyrRS is neutralized with anti-*Ld*TyrRS antibodies (*C*). The binding is also significantly reduced with the mutant *Ld*TyrRS (ELR/AAA) protein (*D*). *E* and *F,* cytokine secretion assays for IL-6 (*E*) and TNF-α (*F*) using mice macrophages and anti-CXCR2 and anti-*Ld*TyrRS antibodies. The secretion of these proinflammatory cytokines is reduced when macrophages and *Ld*TyrRS protein were preincubated with the anti-CXCR2 (*TyrRS* + α-*CXCR2 Ab*) and anti-*Ld*TyrRS (*TyrRS* + α-*TyrRS Ab*) antibodies, respectively. The results represent mean ± S.D. with $n = 3$. Tukey's test was performed, and *p* values are indicated.

it may be hypothesized that secretion of *Ld*TyrRS is a pro-parasitic response that is likely to bring about the recruitment of neutrophils to the site of infection.

Because ELR motif is also involved in a ligand-based interaction with CXCR2 receptors on immune cells, we also analyzed the binding of *Ld*TyrRS to host macrophages. Our confocal and

FACS data show that via its ELR motif, released *Ld*TyrRS interacts with a specific receptor on host macrophages. Our data also indicates that the *Ld*TyrRS-macrophage interaction triggers the release of the proinflammatory cytokines TNF-α and IL-6. Previous studies have shown that *Leishmania* infection triggers the release of TNF-α and IL-6 (38–41). A central function of these two proinflammatory cytokines is to help in the recruitment of phagocytes like neutrophils and monocytes (42–44). Both cell types are infection targets and essential for the establishment of *Leishmania* infection (45–47). In the case of *Leishmania* infections, the release of TNF-α and IL-6 by the parasite secretory protein GP63 has been directly associated with inflammatory phagocyte (neutrophil and monocyte) recruitment (40). Thus, it may be hypothesized that the secretion of TNF-α and IL-6 by *Ld*TyrRS also contributes toward the accrual of neutrophils at the site of *Leishmania* infection. These results clearly indicate that the secreted *Ld*TyrRS enables *Leishmania* to elicit proinflammatory cytokine release and neutrophil recruitment, both of which contribute to the establishment of infection. In our present set of experiments, we observed that 0.1 nM (6 ng) *Ld*TyrRS was sufficient to initiate neutrophil chemotaxis and cytokine release from host cells. This concentration was found to correlate with the amount of protein present in $\sim 2 \times 10^5$ parasites.

During *Leishmania* infection, most sand flies transmit 10^3-10^5 parasites per blood meal (48). Earlier reports indicate that tissue damage to the skin caused by the infected sand fly bites is important to induce neutrophil recruitment within the first 90 min, further indicating that the initial neutrophil recruitment in the case of a natural infection is parasite-independent (46). However, in the case of an experimental infection in mice, a needle injection of 10^5 *Leishmania* parasites is required to observe parasite-dependent neutrophil recruitment at later time points (6–24 h post-infection) (49, 50). Thus, in a natural *Leishmania* infection, apart from parasitic proteins other factors derived from the sand fly also contribute to neutrophil chemotaxis in the infected dermis. Because all these chemotactic factors (both parasite and sandfly derived) work in a synergistic manner, it would be interesting to observe the cooperation between the *Ld*TyrRS and other chemoattractants. Although in the present study, the amount of *Ld*TyrRS used was within the physiological range, the exact amount of protein secreted during natural infection, and the minimal effective concentration required for its chemotactic activity needs to be evaluated by further experimentation.

In summary, our data indicates a possible immunomodulating role of *Ld*TyrRS in *Leishmania* infection. *Ld*TyrRS functions as a direct chemoattractant for neutrophils. *Ld*TyrRS was also found to induce TNF-α and IL-6 release, which is known to be associated with inflammatory phagocyte recruitment in *Leishmania* infections. Improved knowledge of *Leishmania*-induced inflammation will further our understanding of how the parasite establishes infection, modulates the immune response, metastasizes, and causes pathology.

Considering that drug resistance is a major concern in antiparasitic chemotherapy, there is continuous pressure to identify new drug targets. Our comprehensive analyses on the twin abilities of *Leishmania* parasite tyrosyl-tRNA synthetase provide a platform to explore *LdTyrRS* as a potential target for drug development.

Experimental Procedures

Materials—All restriction enzymes and DNA modifying enzymes were obtained from New England Biolabs. Paromomycin and hygromycin were obtained from Sigma. Plasmid pET-30a was obtained from Novagen. *Escherichia coli* DH10β and Rosetta were used as hosts for plasmid cloning and protein expression, respectively. Nickel-nitrilotriacetic acid-agarose was purchased from Qiagen. DNA and protein markers were acquired from New England Biolabs. Resveratrol and fisetin were obtained from Sigma. ELISA kits and antibodies were obtained from BD Bioscience. The rabbit anti-tubulin-α antibody was obtained from Neomarker (Fremont, CA). Other materials used in this study were of analytical grade and were commercially available.

Strains and Culture Conditions—L. donovani Bob (*Ld*Bob/strain/MHOM/SD/62/1SCL2D) was obtained from Dr. Stephen Beverley (Washington University, St. Louis, MO). Wild-type (WT) promastigotes were cultured at 22 °C in M199 medium (Sigma) supplemented with 100 units/ml of penicillin (Sigma), 100 μg/ml of streptomycin (Sigma), and 5% heat-inactivated fetal bovine serum (Gibco). WT parasites were routinely cultured in media with no drug supplementation, whereas genetically manipulated *TyrRS* heterozygotes (*TyrRS*/*HYG*, *TyrRS*/*NEO*) were maintained in either 200 μg/ml of hygromycin or 300 μg/ml of paromomycin, respectively. The *TyrRS* overexpressing (*WT[pTyrRS$^+$]*) parasites were maintained in 800 μg/ml of zeocin. The add-back line *TyrRS/HYG[pTyrRS$^+$]*, was grown in 800 μg/ml of zeocin and 150 μg/ml of hygromycin. For characterization of mutant parasites phenotypically, the cells were subcultured without selection markers prior to experiments.

Axenic amastigotes were generated by using the standard protocol as described earlier (51, 52). Briefly, late-log phase promastigote cultures ($\sim 2 \times 10^6$/ml) were adapted to grow at 26 °C in an acidic amastigote media (RPMI 1640, 25 mM MES, pH 5.5). Once established, these parasites were subsequently grown in acidic medium (RPMI 1640/MES, pH 5.5) at 37 °C in a humidified atmosphere containing 5% CO_2. Throughout this *in vitro* adaptation process, the cellular morphology of the parasites was examined by both phase-contrast light microscopy and Giemsa-stained preparations. The mouse macrophage-like cell line J774.A1 obtained from ATCC was cultured in RPMI 1640 media (Sigma) supplemented with 10% FBS and antibiotics (100 units/ml of penicillin and 100 μg/ml of streptomycin) at 37 °C with 5% CO_2.

Ethics Statement—All animal experiments were performed according to the guidelines approved by the Committee for the Purpose of Control and Supervision of Experiments on Animals (CPCSEA), Ministry of Environment and Forest, Government of India. The protocol was approved by the Institutional Animal Ethics Committee (IAEC) of Jawaharlal Nehru University (JNU), New Delhi (IAEC code number 11/2013). All mice used for the experiments were ethically sacrificed by asphyxiation with carbon dioxide according to the institutional and the CPCSEA (Government of India) regulations.

TABLE 1
Primers used for generation of the Hyg and Neo specific linear replacement cassette fragments

S. No.	*L. donovani* primers	Sequences
1	A	5′-AACATGACGCAGTGGTGTCTCCGTT-3′
2	B_{Hyg}	5′-GGTGAGTTCAGGCTTTTTCATATGCGGCGTGCTCAGCGAACGAAA-3′
3	C_{Hyg}	5′-CGTTTCGTTCGCTGAGCACGCCGCATATGAAAAAGCCTGAACTCA-3′
4	D_{Hyg}	5′-GCCGCCTCTTCACCTATACCCTATTCCTTTGCCCTCGGACGA-3′
5	E_{Hyg}	5′-CTCGTCCGAGGGCAAAGGAATAGGGTATAGGTGAAGAGGCGGC-3′
6.	B_{Neo}	5′-CAATCCATCTTGTTCAATCATATGCGGCGTGCTCAGCGAACGAAA-3′
7	C_{Neo}	5′-CGTTTCGTTCGCTGAGCACGCCGCATATGATTGAACAAGATGGATT-3′
8	D_{Neo}	5′-GCCGCCTCTTCACCTATACCTCAGAAGAACTCGTCAAGAA-3′
9	E_{Neo}	5′-CTTCTTGACGAGTTCTTCTGAGGTATAGGTGAAGAGGCGGC-3′
10	F	5′-GTGGAAGCAAGGGCAACACA-3′
11	G	5′-TTTTTCTAGAATGAACACGGACGACCGCTAC-3′
12	H	5′-TTTTAAGCTTTACCTCTTCTTTGCCATCTTCTTC-3′

Cloning, Expression, and Purification of Recombinant LdTyrRS Protein—The gene for *LdTyrRS* (tritrypDB ID LdBPK_141460.1) was amplified by PCR using a forward primer with a flanking BamHI site (5′-TTTTGGATCCATGAACACGGACGACCGCTAC-3′) and reverse primer with a flanking HindIII site (5′-TTTTAAGCTTTACCTCTTCTTTGCCATCTTCTTC-3′) from *L. donovani* genomic DNA. The 2049-bp amplification product encompassing the *LdTyrRS* open reading frame (ORF) was cloned into a pET30a vector (Novagen) using BamHI and HindIII restriction sites. This construct (*LdTyrRS*-pET30a) containing a His_6 tag at the N terminus was transformed into the *E. coli* Rosetta strain (Novagen). The expression of recombinant *Ld*TyrRS (r*Ld*TyrRS) was induced with 0.5 mM isopropyl β-D-thiogalactopyranoside at 18 °C for 16 h. The protein was purified by a Ni^{2+}-nitrilotriacetic acid-agarose resin (Qiagen) by eluting with increasing concentrations of imidazole. The purified protein was found to be >95% pure as judged by SDS-PAGE.

Site-directed Mutagenesis of the ELR Peptide Motif of LdTyrRS—The ELR motif of *Ld*TyrRS was replaced with AAA by site-directed mutagenesis. The mutation in the *LdTyrRS* gene was performed using the QuikChange II site-directed mutagenesis kit (Agilent Technologies, USA) following the manufacturer's instructions. Subsequently, a DNA sequence analysis was performed to confirm the mutations. The mutated recombinant protein (ELR/AAA) was expressed and purified using the same protocol as specified above for the recombinant WT *Ld*TyrRS.

Aminoacylation Spectrophotometric Assay—The aminoacylation assays were performed as previously described (53). Briefly, the substrate *L. donovani* $tRNA^{Tyr}$ was synthesized by *in vitro* transcription from a PCR product template that contained a T7 promoter followed by the *L. donovani* $tRNA^{Tyr}$ sequence (tritrypDB ID LinJ.34.tRNA7) and the terminal CCA sequence. The *in vitro* transcription reaction was performed with the MEGAScript T7 polymerase kit (Ambion; Life Technologies) according to the manufacturer's instructions. The reaction mixtures were then extracted with phenol/chloroform/isoamyl alcohol (25:24:1 (v/v), Sigma), and the tRNAs were precipitated with isopropyl alcohol (Sigma). The tRNA was refolded by heating at 70 °C for 10 min, followed by the addition of 10 mM $MgCl_2$ and slow cooling to room temperature. The aminoacylation reaction was performed as described earlier (53) in 30 mM Hepes (pH 7.5), 150 mM NaCl, 30 mM KCl, 50 mM $MgCl_2$, 1 mM DTT, 200 μM ATP, 10 mM L-tyrosine, 8 μM $tRNA^{Tyr}$, 2 units/ml of inorganic pyrophosphatase (Sigma), and 0.2 μM r*Ld*TyrRS protein at 37 °C. The reaction was stopped at different time points by the addition of 10 mM EDTA and developed by malachite green (Echelon Bioscience). The absorbance was then measured at 620 nm by a Spectramax M2 reader (Molecular Devices). The determination of K_m and V_{max} for L-tyrosine and $tRNA^{Tyr}$ was achieved by varying the concentration of L-tyrosine or $tRNA^{Tyr}$ in the reaction mixture while maintaining the other components in excess. To determine the effect of the inhibitors on the aminoacylation activity of r*Ld*TyrRS, reactions were performed in the presence of inhibitors as described previously (53). Briefly, a reaction mixture containing r*Ld*TyrRS (0.2 μM) was incubated with different concentrations of fisetin/resveratrol (0.1 nM to 1000 μM) for 30 min at 37 °C. The reactions were stopped and quantitated as described above. To determine the 50% inhibitory concentration (IC_{50}), the dose-response data were fitted to the log (inhibitor) *versus* response equation using GraphPad Prism.

Molecular Constructs for Replacement of TyrRS Alleles—For inactivation of the *LdTyrRS* gene, a targeted gene replacement strategy based on PCR fusion was employed (54). Briefly, the flanking regions of the *TyrRS* gene (5′-UTR and 3′-UTR) were amplified and fused by PCR to the hygromycin phosphotransferase gene (*HYG*) or neomycin phosphotransferase gene (*NEO*). The 5′-UTR (599 bp) of the *LdTyrRS* gene was obtained from WT *L. donovani* genomic DNA by PCR amplification with either primer A and B_{Hyg} or primers A and B_{Neo} (Table 1). The *NEO* gene was amplified from pX63-NEO with primers C_{Neo} and D_{Neo}. The *HYG* gene was amplified from pX63-HYG with primers C_{Hyg} and D_{Hyg} (Table 1). The 3′-UTR (580 bp) of the *LdTyrRS* gene was obtained from *L. donovani* WT genomic DNA by PCR amplification using primers E_{Hyg}/E_{Neo} and reverse primer F (Table 1). The 5′-UTR of *L. donovani TyrRS* gene was then ligated to either of the antibiotic resistance marker genes (*HYG*/*NEO*) by PCR using primers A and D_{Hyg} or A and D_{Neo}. This fragment (5′-UTR marker gene) was then fused with the 3′-UTR using primers A and F, yielding the linear replacement cassette, 5′UTR-Hyg-3′UTR or 5′UTR-Neo-3′UTR.

To generate the episomal construct, the full-length *LdTyRS* coding sequence was amplified with a forward primer harboring the XbaI site (primer G) and a reverse primer with the HindIII site (primer H) (Table 1). The amplified *LdTyRS* gene was

TABLE 2
Primers used for the molecular characterization of the genetically manipulated parasites by PCR-based analysis

S. No.	*L. donovani* primers	Sequences
1	Primer 1	5′-TGTAGAAGTACTCGCCGATAGTGG-3′
2	Primer 2	5′-AGATCGCATTGCAGCACAGC-3′
3	Primer 3	5′-CGCAGCTATTTACCCGCAGGACAT-3′
4	Primer 4	5′-CGTCGTCATTTCCGCCTTACGC-3′
5	Primer 5	5′-ATAGCGTTGG CTACCCGTGATATTGC-3′
6	Primer 6	5′-AACACGGCGGCATCAGAGCAGCCGATTG-3′
7	Primer 7	5′-GAAGAAGATGGCAAAGAAGAGGTAA-3′
8	Primer 8	5′-GCGGTCGTCCGTGTTCAT-3′

then cloned into the pSP72α-zeo-α vector to get the pSP72α-zeo-α-TyRS episomal construct. All the fragments and constructs were sequenced for confirmation.

Generation of Genetically Manipulated Parasites—After PCR amplification and purification, ~2 μg of the linear replacement cassette (5′UTR-Hyg-3′UTR or 5′-UTR-Neo-3′UTR) was individually transfected by electroporation in WT *L. donovani* promastigotes (55). The transfectants were subjected to antibiotic selection depending on the marker gene. The cells resistant to antibiotic selection were further subjected to PCR-based analysis to check for the correct integration of replacement cassettes using primers as shown in Table 2. Thereafter, the second round of transfection was initiated to knockout the other allele of the *TyrRS* gene.

To generate the episomal complementation mutants, the episomal construct (pSP72α-zeo-α-TyrRS) was transfected into the heterozygous *TyrRS*/*HYG* parasites to get the add-back line (*TyrRS*/*HYG*[*pTyrRS*$^+$*J*). The wild-type promastigotes were also transfected with the episomal construct (pSP72α-zeo-α-TyrRS) to generate the overexpressing (*WT[pTyrRS*$^+$]) mutant parasites. The correct integration was confirmed by PCR (data not shown) and Western blotting analysis.

Growth and Infectivity Assays—Growth rate experiments were conducted by inoculating stationary phase parasites at a density of 1×10^6 cells/ml in M199 medium with 5% FBS in 25-cm^2 flasks without respective selection drug at 22 °C. The growth rate of each culture was determined at 24-h intervals with a Neubauer hemocytometer. Growth studies with individual cell lines were done at least three times, and similar results were consistently obtained.

For the infectivity assay, the J774.A1 murine macrophage cell line was plated at a cell density of 5×10^5 cell/well in a 6-well flat bottom plate. The adherent cells were infected with stationary phase promastigotes, at a ratio of 20:1 for 6 h. Excess non-adherent promastigotes were then removed by incubating the cells for 30 s in phosphate-buffered saline (PBS). These were then subsequently maintained in RPMI 1640 media containing 10% FBS at 37 °C with 5% CO_2. Giemsa staining was performed to visualize the intracellular parasite load.

Drug Sensitivity Assay—To determine the effect of inhibitors (resveratrol and fisetin) on the viability of *L. donovani* promastigote cells a colorimetric 3-(4,5-dimethylthiazol-2-yl)-2,5-diphenyltetrazolium bromide assay was performed as described previously (56). Briefly, log phase promastigotes (5×10^4 cells/well) were seeded in a 96-well flat-bottomed plate (Nunc) and incubated with different inhibitor concentrations at 22 °C. Because the inhibitors were dissolved in DMSO, a sample without inhibitors but with an equal volume of DMSO served as an additional control. After 72 h of incubation, 10 μl of 3-(4,5-dimethylthiazol-2-yl)-2,5-diphenyltetrazolium bromide (5 mg/ml) was added to each well and the plates were further incubated at 37 °C for 4 h. The reaction was stopped by the addition of 50 μl of 50% isopropyl alcohol and 20% SDS followed by gentle shaking at 37 °C for 30 min to 1 h. The absorbance was measured at 570 nm in a microplate reader (SpectraMax M2 from Molecular Devices). The percentage of parasite growth at different inhibitor concentrations was determined relative to untreated control cells and 50% inhibitory concentration (IC_{50}) was calculated.

The sensitivity of amastigotes to fisetin and resveratrol was tested in an intracellular amastigote-macrophage model as described earlier (57). Briefly, the J774A.1 cell line (1×10^5 cells/well) was cultured in eight-chamber Lab-Tek tissue culture slides (Nunc, USA) and infected with stationary phase promastigotes at an multiplicity of infection of 20:1 as described above. The infected macrophages were then incubated for 72 h with different concentrations of inhibitors (0.1 nM to 10,000 μM). The slides were fixed and stained with Giemsa. The number of amastigotes per cell was counted in 100 macrophages at different drug concentrations. The 50% inhibitory concentration (IC_{50}) was obtained by determining the reduction in parasite burden relative to the untreated infected controls.

Antibody Generation and Immunofluorescence Microscopy—Antibodies against the r*Ld*TyrRS were raised commercially in rabbits (Merck). Briefly, the purified r*Ld*TyrRS protein (50 μg) was subcutaneously injected in rabbit using Freund's complete adjuvant (Sigma), followed by three booster doses of the recombinant protein (20 μg) in Freund's incomplete adjuvant (Sigma), at a 2-week interval. The sera were then collected after the last booster. Protein A-purified IgG fractions (anti-*Ld*TyrRS antibody) were utilized for further immunological assays.

For the intracellular localization of *Ld*TyrRS, *L. donovani* promastigotes were immobilized on poly-L-lysine-coated coverslips. The cells were fixed and permeabilized followed by incubation with the anti-*Ld*TyrRS antibody (1:1000) for 1 h at room temperature. Subsequently, the cells were washed and then incubated for 45 min with the Alexa 546-conjugated goat anti-rabbit IgG antibody (Thermo Fisher Scientific catalogue number A-11071). The nuclear and the kinetoplastid DNA was stained with DAPI (Invitrogen). The fluorescence of the parasites stained with the anti-*Ld*TyrRS antibody was visualized by a confocal laser scanning microscope (Olympus FluoView^{TM} FV1000 with objective lenses PLAPON ×60 O, NA-1.42) at an excitation wavelength of 556 nm. The cellular DNA stained with DAPI was visualized at an excitation wavelength of 405 nm.

Immunofluorescence analysis of the infected macrophages was performed as previously described (58). Briefly, J774 cells (1×10^5) were grown on coverslips in RPMI 1640 supplemented with 10% FBS. The adherent cells were then infected with *L. donovani* stationary-phase promastigotes at an multiplicity of infection of 20:1 or left uninfected. After 24 h of infection, the cells were fixed and permeabilized followed by incu-

bation with the primary (anti-*Ld*TyrRS and secondary (Alexa 488-conjugated goat anti-rabbit IgG) antibodies. All antibody incubations were of 50 min duration and were followed by six to eight washes in PBS. The images were then visualized by the confocal laser scanning microscope (Olympus FluoView™ FV1000 with objective lenses PLAPON ×60 O, NA-1.42) at an excitation wavelength of 495 nm. DAPI was used to stain the nuclei of both the parasite and host macrophages.

Immunoprecipitation and Western Blotting Analysis—Immunoprecipitation of the *Ld*TyrRS was performed using the culture supernatants as previously described (58). Briefly, the culture supernatants from uninfected macrophages, infected macrophages, and promastigote cultures were collected by centrifugation. The culture supernatants were neutralized with 5 N NaOH and concentrated using an Amicon Ultra-15 centrifugal filter unit (Millipore). The concentrated culture supernatants were incubated overnight at 4 °C with anti-*Ld*TyrRS antibodies. Protein A-Sepharose beads (Sigma) were then added to each sample for 30 min, following which the beads were washed with *Leishmania* lysis buffer (50 mM Tris, pH 8, 137 mM NaCl, complete protease inhibitor mixture (Roche)). The immunoprecipitated proteins were eluted from the beads using 0.2 M glycine buffer. SDS-PAGE was used to separate the eluted immunoprecipitated proteins from the culture supernatant, which were then detected by Western blotting analysis.

Protein samples for Western blotting analysis were fractionated on a 10% SDS-PAGE gel and blotted onto a nitrocellulose membrane using electrophoretic transfer cell (Bio-Rad). After blocking with 5% skimmed milk, the membrane was incubated for 2 h at room temperature with the anti-*Ld*TyrRS antibody (1:1000). The membrane was then washed with PBS containing 0.05% Tween 20 (PBS-T) and incubated with the horseradish peroxidase (HRP)-conjugated anti-rabbit antibody (Cell Signaling Technology, catalogue number 7076S; 1:5000). The blot was developed by the enhanced chemiluminescence (ECL®) kit (Amersham Biosciences) according to the manufacturer's protocol.

The quantification of *Ld*TyrRS in the immunoblot was carried out as described earlier (59, 60). Briefly, different concentrations of r*Ld*TyrRS were analyzed using anti-*Ld*TyrRS antibody by Western blotting analysis. Band intensities for r*Ld*TyrRS were measured densitometrically. A standard curve of protein load *versus* band intensity was then produced (data not shown). The band intensity of *Ld*TyrRS from the parasite lysate was calibrated against the standard curve generated for the recombinant protein. 30 ng of *Ld*TyrRS was estimated to be present in $\sim 10^6$ parasites. In our present set of experiments with mammalian cells, the minimum quantity of *Ld*TyrRS used was 6 ng, which is equivalent to the amount of protein present in $\sim 2 \times 10^5$ *Leishmania* parasites. Because the experimental infections in mice are done using 10^5-10^7 *Leishmania* parasites (49, 61), it would appear that the amount of *Ld*TyrRS (6 ng) used is within the physiological range.

Chemotaxis Assays—For the neutrophil chemotactic assay, mice neutrophils were isolated with a Ficoll-Paque (Sigma) centrifugation method, as previously described (62). The final preparation consisted of >98% neutrophils, as determined by Wright-Giemsa staining. The cells were resuspended in chemotaxis media (RPMI 1640 containing 10% FBS) at a concentration of 5×10^6 cells/ml. 200 μl of this cell suspension (1×10^6 cells) was plated in the upper well of a 24-well transwell Boyden chemotaxis plate (Costar). Recombinant *Ld*TyrRS (0.1 nM or 6 ng), fMLP (10^{-8} M), and mutant *Ld*TyrRS protein (ELR/AAA) (0.1 nM or 6 ng) were diluted in 600 μl of the chemotaxis medium and placed in the lower well. The filled chemotaxis transwell plates were then incubated at 37 °C in a humidified CO_2 incubator for 4 h. After the incubation, non-migratory cells on the upper surface of the filter were removed by wiping with a cotton swab. The number of neutrophils that migrated into the lower chamber was determined. For quantification, the myeloperoxidase activity of neutrophils was measured as previously described (63). Briefly, neutrophils sedimented by light centrifugation were solubilized in 0.1% Triton X-100. To this lysate, 300 μl of the *o*-dianisidine solution containing 0.003% sodium perborate was added. The color of the reaction was developed for 30 min and terminated by the addition of 50 μl of 0.5 N HCl. The absorbance of the reaction was measured at 405 nm. The number of neutrophils that migrated to the lower chamber was calculated from a standard curve obtained with the lysates of a known number of neutrophils. Migration was plotted either as the mean number of neutrophils migrated in the lower chamber or as migration index (MI = number of migrating cells in each condition/number of migrating cells in basal medium).

Cell Binding Assays—In vitro binding of the r*Ld*TyrRS to mouse macrophages was performed by immunofluorescence analysis using standard protocols. The murine macrophage cell line J774 was cultured on coverslips in 6-well plates and maintained in RPMI 1640 medium containing 10% FBS. Recombinant *Ld*TyrRS (0.1 nM or 6 ng) and mutant *Ld*TyrRS protein (0.1 nM or 6 ng) (ELR/AAA) were incubated with the cells for 2 h at 4 °C. The cells were then washed and incubated with 2% paraformaldehyde (Sigma) for 15 min. Following this, the primary (anti-*Ld*TyrRS, 1:1000) and fluorescently conjugated secondary (Thermo Fisher Scientific catalogue number A-11071, 1:3000) antibodies were added. Fluorescence microscopy was performed with confocal laser scanning microscopy (Olympus FluoView™ FV1000 with objective lenses PLAPON ×60 O, NA-1.42).

In vitro binding of the r*Ld*TyrRS to J774 cells was also analyzed by fluorescence-activated cell sorting (FACS) using standard protocols. Analytical flow cytometry was performed by indirect staining of the macrophages with the anti-*Ld*TyrRS antibody (1:1000) and the fluorescently conjugated secondary antibodies (Thermo Fisher Scientific, catalogue number A-11071; 1:3000). The data obtained on BD FACS Calibur (BD Biosciences) were analyzed using CellQuest software.

Cytokine Secretion Assays—The concentrations of IL-6, TNF-α, IL-12, IFN-γ, and IL-10 in culture supernatants were determined by ELISA. Briefly, J774 murine macrophages (5×10^5) were cultured in RPMI 1640 medium with 10% FBS in 24-well plates. LPS, r*Ld*TyrRS, and control proteins (r*Ld*TyrRS mutant protein (ELR/AAA) and r*Ld*LeuRS) were added to the cells at different concentrations. After 6, 12, and 24 h, the culture supernatants were collected, serially diluted, and the cytokine concentrations were quantified by ELISA. The assay was

performed using a BD Pharmingen Opt EIA kit according to the manufacturer's instructions. To remove endotoxin contamination, recombinant proteins (r*Ld*TyrRS, r*Ld*TyrRS mutant protein (ELR/AAA), and r*Ld*LeuRS) were passed through polymyxin beads (Sigma) before the assay. To confirm that the proteins were endotoxin-free, a LAL (limulus amebocyte lysate) assay (Thermo Fisher Scientific catalogue number 88282) was performed.

LdTyrRS Interaction with Murine Macrophages—J774 murine macrophages (5×10^5) were cultured with r*Ld*TyrRS in the absence or presence of different antibodies (anti-*Ld*TyrRS or anti-CXCR2). Binding of r*Ld*TyrRS was then tested by using a standard FACS protocol as described above. In related experiments, the cytokine profiling of these murine macrophages was also done. The cytokines released in the culture supernatants were detected by ELISA using commercially available kits according to the manufacturer's protocol (BD Pharmingen Opt EIA).

Statistical Analysis—Results for the aminoacylation activity, parasitemia, and the neutrophil migration index were entered as column data in GraphPad Prism and analyzed using Student's *t* test. Results for cytokine analysis were entered as grouped data in GraphPad Prism 5 and analyzed by two-way analysis of variance followed by Tukey's multiple comparison post test. The data are represented as mean ± S.D. A p value of < 0.05 was accepted as an indication of statistical significance.

Author Contributions—S. A. conducted the experiments. R. M. B. designed the study, supervised the experiments, and edited the manuscript with contributions from S. A. Both the authors reviewed the manuscript.

Acknowledgments—We thank the Central Instrumentation Facility at the School of Life Sciences, Jawaharlal Nehru University, for MALDI-TOF analysis and for providing the imaging facility. We are grateful to Dr. Chandrima Saha for providing the Leishmania mitochondrial tryparedoxin peroxidise (mTXNPX) antibody.

References

1. Guo, M., and Schimmel, P. (2013) Essential nontranslational functions of tRNA synthetases. *Nat. Chem. Biol.* **9,** 145–153
2. Park, S. G., Ewalt, K. L., and Kim, S. (2005) Functional expansion of aminoacyl-tRNA synthetases and their interacting factors: new perspectives on housekeepers. *Trends Biochem. Sci.* **30,** 569–574
3. Guo, M., Yang, X. L., and Schimmel, P. (2010) New functions of aminoacyl-tRNA synthetases beyond translation. *Nat. Rev. Mol. Cell Biol.* **11,** 668–674
4. Wakasugi, K., and Schimmel, P. (1999) Two distinct cytokines released from a human aminoacyl-tRNA synthetase. *Science* **284,** 147–151
5. Wakasugi, K., and Schimmel, P. (1999) Highly differentiated motifs responsible for two cytokine activities of a split human tRNA synthetase. *J. Biol. Chem.* **274,** 23155–23159
6. Strieter, R. M., Polverini, P. J., Kunkel, S. L., Arenberg, D. A., Burdick, M. D., Kasper, J., Dzuiba, J., Van Damme, J., Walz, A., and Marriott, D. (1995) The functional role of the ELR motif in CXC chemokine-mediated angiogenesis. *J. Biol. Chem.* **270,** 27348–27357
7. Addison, C. L., Daniel, T. O., Burdick, M. D., Liu, H., Ehlert, J. E., Xue, Y. Y., Buechi, L., Walz, A., Richmond, A., and Strieter, R. M. (2000) The CXC chemokine receptor 2, CXCR2, is the putative receptor for ELR^+ CXC chemokine-induced angiogenic activity. *J. Immunol.* **165,** 5269–5277
8. Stillie, R., Farooq, S. M., Gordon, J. R., and Stadnyk, A. W. (2009) The functional significance behind expressing two IL-8 receptor types on PMN. *J. Leukoc. Biol.* **86,** 529–543
9. Graves, D. T., and Jiang, Y. (1995) Chemokines, a family of chemotactic cytokines. *Crit. Rev. Oral Biol. Med.* **6,** 109–118
10. Kaye, P., and Scott, P. (2011) Leishmaniasis: complexity at the host-pathogen interface. *Nat. Rev. Microbiol.* **9,** 604–615
11. Cecílio, P., Pérez-Cabezas, B., Santarém, N., Maciel, J., Rodrigues, V., and Cordeiro da Silva, A. (2014) Deception and manipulation: the arms of *Leishmania*, a successful parasite. *Front. Immunol.* **5,** 480
12. Croft, S. L., Sundar, S., and Fairlamb, A. H. (2006) Drug resistance in leishmaniasis. *Clin. Microbiol. Rev.* **19,** 111–126
13. Larson, E. T., Kim, J. E., Castaneda, L. J., Napuli, A. J., Zhang, Z., Fan, E., Zucker, F. H., Verlinde, C. L., Buckner, F. S., Van Voorhis, W. C., Hol, W. G., and Merritt, E. A. (2011) The double-length tyrosyl-tRNA synthetase from the eukaryote *Leishmania major* forms an intrinsically asymmetric pseudo-dimer. *J. Mol. Biol.* **409,** 159–176
14. Gowri, V. S., Ghosh, I., Sharma, A., and Madhubala, R. (2012) Unusual domain architecture of aminoacyl tRNA synthetases and their paralogs from *Leishmania major*. *BMC Genomics* **13,** 621
15. Baggiolini, M., and Clark-Lewis, I. (1992) Interleukin-8, a chemotactic and inflammatory cytokine. *FEBS Lett.* **307,** 97–101
16. Jia, J., Li, B., Jin, Y., and Wang, D. (2003) Expression, purification, and characterization of human tyrosyl-tRNA synthetase. *Protein Expr. Purif.* **27,** 104–108
17. Kijima, S., Ohta, T., and Imahori, K. (1968) Purification and characterization of tyrosyl-RNA synthetase from baker's yeast. *J. Biochem.* **63,** 434–445
18. Cestari, I., Kalidas, S., Monnerat, S., Anupama, A., Phillips, M. A., and Stuart, K. (2013) A multiple aminoacyl-tRNA synthetase complex that enhances tRNA-aminoacylation in African trypanosomes. *Mol. Cell. Biol.* **33,** 4872–4888
19. Sajish, M., and Schimmel, P. (2015) A human tRNA synthetase is a potent PARP1-activating effector target for resveratrol. *Nature* **519,** 370–373
20. Silverman, J. M., Chan, S. K., Robinson, D. P., Dwyer, D. M., Nandan, D., Foster, L. J., and Reiner, N. E. (2008) Proteomic analysis of the secretome of *Leishmania donovani*. *Genome Biol.* **9,** R35
21. Gadelha, F. R., Gonçalves, C. C., Mattos, E. C., Alves, M. J., Piñeyro, M. D., Robello, C., and Peloso, E. F. (2013) Release of the cytosolic tryparedoxin peroxidase into the incubation medium and a different profile of cytosolic and mitochondrial peroxiredoxin expression in H_2O_2-treated *Trypanosoma cruzi* tissue culture-derived trypomastigotes. *Exp. Parasitol.* **133,** 287–293
22. Laskay, T., van Zandbergen, G., and Solbach, W. (2003) Neutrophil granulocytes: trojan horses for *Leishmania major* and other intracellular microbes? *Trends Microbiol.* **11,** 210–214
23. Chandrasekar, B., Melby, P. C., Sarau, H. M., Raveendran, M., Perla, R. P., Marelli-Berg, F. M., Dulin, N. O., and Singh, I. S. (2003) Chemokine-cytokine cross-talk. The ELR^+ CXC chemokine LIX (CXCL5) amplifies a proinflammatory cytokine response via a phosphatidylinositol 3-kinase-NF-κB pathway. *J. Biol. Chem.* **278,** 4675–4686
24. Bhatt, T. K., Khan, S., Dwivedi, V. P., Banday, M. M., Sharma, A., Chandele, A., Camacho, N., Ribas de Pouplana, L., Wu, Y., Craig, A. G., Mikkonen, A. T., Maier, A. G., Yogavel, M., and Sharma, A. (2011) Malaria parasite tyrosyl-tRNA synthetase secretion triggers pro-inflammatory responses. *Nat. Commun.* **2,** 530
25. Gupta, G., Bhattacharjee, S., Bhattacharyya, S., Bhattacharya, P., Adhikari, A., Mukherjee, A., Bhattacharyya Majumdar, S., and Majumdar, S. (2009) CXC chemokine-mediated protection against visceral leishmaniasis: involvement of the proinflammatory response. *J. Infect. Dis.* **200,** 1300–1310
26. Kane, M. M., and Mosser, D. M. (2001) The role of IL-10 in promoting disease progression in leishmaniasis. *J. Immunol.* **166,** 1141–1147
27. Gupta, G., Oghumu, S., and Satoskar, A. R. (2013) Mechanisms of immune evasion in leishmaniasis. *Adv. Appl. Microbiol.* **82,** 155–184
28. Matte, C., and Olivier, M. (2002) *Leishmania*-induced cellular recruitment during the early inflammatory response: modulation of proinflammatory mediators. *J. Infect. Dis.* **185,** 673–681
29. Silverman, J. M., Clos, J., de'Oliveira, C. C., Shirvani, O., Fang, Y., Wang, C.,

Foster, L. J., and Reiner, N. E. (2010) An exosome-based secretion pathway is responsible for protein export from *Leishmania* and communication with macrophages. *J. Cell Sci.* **123,** 842–852
30. Brown, M. V., Reader, J. S., and Tzima, E. (2010) Mammalian aminoacyl-tRNA synthetases: cell signaling functions of the protein translation machinery. *Vascul. Pharmacol.* **52,** 21–26
31. Wakasugi, K., Slike, B. M., Hood, J., Otani, A., Ewalt, K. L., Friedlander, M., Cheresh, D. A., and Schimmel, P. (2002) A human aminoacyl-tRNA synthetase as a regulator of angiogenesis. *Proc. Natl. Acad. Sci. U.S.A.* **99,** 173–177
32. Park, S. G., Kim, H. J., Min, Y. H., Choi, E. C., Shin, Y. K., Park, B. J., Lee, S. W., and Kim, S. (2005) Human lysyl-tRNA synthetase is secreted to trigger proinflammatory response. *Proc. Natl. Acad. Sci. U.S.A.* **102,** 6356–6361
33. Castro de Moura, M., Miro, F., Han, J. M., Kim, S., Celada, A., and Ribas de Pouplana, L. (2011) Entamoeba lysyl-tRNA synthetase contains a cytokine-like domain with chemokine activity towards human endothelial cells. *PLoS Negl. Trop. Dis.* **5,** e1398
34. Lambertz, U., Silverman, J. M., Nandan, D., McMaster, W. R., Clos, J., Foster, L. J., and Reiner, N. E. (2012) Secreted virulence factors and immune evasion in visceral leishmaniasis. *J. Leukoc. Biol.* **91,** 887–899
35. van Zandbergen, G., Hermann, N., Laufs, H., Solbach, W., and Laskay, T. (2002) *Leishmania* promastigotes release a granulocyte chemotactic factor and induce interleukin-8 release but inhibit γ interferon-inducible protein 10 production by neutrophil granulocytes. *Infect. Immun.* **70,** 4177–4184
36. Laufs, H., Müller, K., Fleischer, J., Reiling, N., Jahnke, N., Jensenius, J. C., Solbach, W., and Laskay, T. (2002) Intracellular survival of *Leishmania major* in neutrophil granulocytes after uptake in the absence of heat-labile serum factors. *Infect. Immun.* **70,** 826–835
37. Aga, E., Katschinski, D. M., van Zandbergen, G., Laufs, H., Hansen, B., Müller, K., Solbach, W., and Laskay, T. (2002) Inhibition of the spontaneous apoptosis of neutrophil granulocytes by the intracellular parasite *Leishmania major*. *J. Immunol.* **169,** 898–905
38. Arena, A., Capozza, A. B., Delfino, D., and Iannello, D. (1997) Production of TNF α and interleukin 6 by differentiated U937 cells infected with *Leishmania major*. *New Microbiol.* **20,** 233–240
39. Wenzel, U. A., Bank, E., Florian, C., Förster, S., Zimara, N., Steinacker, J., Klinger, M., Reiling, N., Ritter, U., and van Zandbergen, G. (2012) *Leishmania major* parasite stage-dependent host cell invasion and immune evasion. *FASEB J.* **26,** 29–39
40. Arango Duque, G., Fukuda, M., Turco, S. J., Stäger, S., and Descoteaux, A. (2014) *Leishmania* promastigotes induce cytokine secretion in macrophages through the degradation of synaptotagmin XI. *J. Immunol.* **193,** 2363–2372
41. Karam, M. C., Hamdan, H. G., Abi Chedid, N. A., Bodman-Smith, K. B., Eales-Reynolds, L. J., and Baroody, G. M. (2006) *Leishmania major*: low infection dose causes short-lived hyperalgesia and cytokines upregulation in mice. *Exp. Parasitol.* **113,** 168–173
42. Griffin, G. K., Newton, G., Tarrio, M. L., Bu, D. X., Maganto-Garcia, E., Azcutia, V., Alcaide, P., Grabie, N., Luscinskas, F. W., Croce, K. J., and Lichtman, A. H. (2012) IL-17 and TNF-α sustain neutrophil recruitment during inflammation through synergistic effects on endothelial activation. *J. Immunol.* **188,** 6287–6299
43. Fielding, C. A., McLoughlin, R. M., McLeod, L., Colmont, C. S., Najdovska, M., Grail, D., Ernst, M., Jones, S. A., Topley, N., and Jenkins, B. J. (2008) IL-6 regulates neutrophil trafficking during acute inflammation via STAT3. *J. Immunol.* **181,** 2189–2195
44. Vieira, S. M., Lemos, H. P., Grespan, R., Napimoga, M. H., Dal-Secco, D., Freitas, A., Cunha, T. M., Verri, W. A., Jr., Souza-Junior, D. A., Jamur, M. C., Fernandes, K. S., Oliver, C., Silva, J. S., Teixeira, M. M., and Cunha, F. Q. (2009) A crucial role for TNF-α in mediating neutrophil influx induced by endogenously generated or exogenous chemokines, KC/CXCL1 and LIX/CXCL5. *Br. J. Pharmacol.* **158,** 779–789
45. Ribeiro-Gomes, F. L., and Sacks, D. (2012) The influence of early neutrophil-*Leishmania* interactions on the host immune response to infection. *Front. Cell Infect. Microbiol.* **2,** 59
46. Peters, N. C., Egen, J. G., Secundino, N., Debrabant, A., Kimblin, N., Kamhawi, S., Lawyer, P., Fay, M. P., Germain, R. N., and Sacks, D. (2008) *In vivo* imaging reveals an essential role for neutrophils in leishmaniasis transmitted by sand flies. *Science* **321,** 970–974
47. Ribeiro-Gomes, F. L., Roma, E. H., Carneiro, M. B., Doria, N. A., Sacks, D. L., and Peters, N. C. (2014) Site-dependent recruitment of inflammatory cells determines the effective dose of *Leishmania major*. *Infect. Immun.* **82,** 2713–2727
48. Hurrell, B. P., Regli, I. B., and Tacchini-Cottier, F. (2016) Different *Leishmania* species drive distinct neutrophil functions. *Trends Parasitol.* **32,** 392–401
49. Hurrell, B. P., Schuster, S., Grün, E., Coutaz, M., Williams, R. A., Held, W., Malissen, B., Malissen, M., Yousefi, S., Simon, H. U., Müller, A. J., and Tacchini-Cottier, F. (2015) Rapid Sequestration of *Leishmania mexicana* by neutrophils contributes to the development of chronic lesion. *PLoS Pathog.* **11,** e1004929
50. Thalhofer, C. J., Chen, Y., Sudan, B., Love-Homan, L., and Wilson, M. E. (2011)) Leukocytes infiltrate the skin and draining lymph nodes in response to the protozoan *Leishmania infantum* chagasi. *Infect. Immun.* **79,** 108–117
51. Mittra, B., Cortez, M., Haydock, A., Ramasamy, G., Myler, P. J., and Andrews, N. W. (2013) Iron uptake controls the generation of *Leishmania* infective forms through regulation of ROS levels. *J. Exp. Med.* **210,** 401–416
52. Debrabant, A., Joshi, M. B., Pimenta, P. F., and Dwyer, D. M. (2004) Generation of *Leishmania donovani* axenic amastigotes: their growth and biological characteristics. *Int. J. Parasitol.* **34,** 205–217
53. Cestari, I., and Stuart, K. (2013) A spectrophotometric assay for quantitative measurement of aminoacyl-tRNA synthetase activity. *J. Biomol. Screen.* **18,** 490–497
54. Darveau, A., Pelletier, A., and Perreault, J. (1995) PCR-mediated synthesis of chimeric molecules. *Methods Neurosci.* **26,** 77–85
55. Kapler, G. M., Coburn, C. M., and Beverley, S. M. (1990) Stable transfection of the human parasite *Leishmania major* delineates a 30-kilobase region sufficient for extrachromosomal replication and expression. *Mol. Cell. Biol.* **10,** 1084–1094
56. Mosmann, T. (1983) Rapid colorimetric assay for cellular growth and survival: application to proliferation and cytotoxicity assays. *J. Immunol. Methods* **65,** 55–63
57. Kansal, S., Tandon, R., Dwivedi, P., Misra, P., Verma, P. R., Dube, A., and Mishra, P. R. (2012) Development of nanocapsules bearing doxorubicin for macrophage targeting through the phosphatidylserine ligand: a system for intervention in visceral leishmaniasis. *J. Antimicrob. Chemother.* **67,** 2650–2660
58. McCall, L. I., and Matlashewski, G. (2010) Localization and induction of the A2 virulence factor in *Leishmania*: evidence that A2 is a stress response protein. *Mol. Microbiol.* **77,** 518–530
59. Krobitsch, S., Brandau, S., Hoyer, C., Schmetz, C., Hübel, A., and Clos, J. (1998) *Leishmania donovani* heat shock protein 100: characterization and function in amastigote stage differentiation. *J. Biol. Chem.* **273,** 6488–6494
60. Taylor, S. C., and Posch, A. (2014) The design of a quantitative Western blot experiment. *Biomed. Res. Int.* **2014,** 361590
61. Rolão, N., Melo, C., and Campino, L. (2004) Influence of the inoculation route in BALB/c mice infected by *Leishmania infantum*. *Acta Trop.* **90,** 123–126
62. Luo, Y., and Dorf, M. E. (2001) Isolation of mouse neutrophils. *Curr. Protoc. Immunol.* **Chapter 3,** Unit 3 20
63. Kawa, S., Kimura, S., Hakomori, S., and Igarashi, Y. (1997) Inhibition of chemotactic motility and trans-endothelial migration of human neutrophils by sphingosine 1-phosphate. *FEBS Lett.* **420,** 196–200